United Aircraft Research Laboratories

UNITED AIRCRAFT CORPORATION

EAST HARTFORD, CONNECTICUT 06108

L-990929-3

Measurements of the UV and VUV
Transmission of Optical Materials
During High-Energy Electron Irradiation

NASA Contract No. SNPC-70

REPORTED BY G. E. Palma
G. E. Palma

APPROVED BY Ronald M. Gagosz
R. M. Gagosz,
Senior Research Engineer,
Optical Systems

R. Hecht
R. Hecht, Chief
Instrumentation Laboratory

DATE September 1972

NO. OF PAGES 51

COPY NO. 27

FOREWORD

An exploratory experimental and theoretical investigation of gaseous nuclear rocket technology was conducted by the United Aircraft Research Laboratories under Contract SNPC-70 with the joint AEC-NASA Space Nuclear Systems Office. The Technical Supervisors of the Contract for NASA were Captain C. E. Franklin (USAF) of SNSO for the initial portion of the Contract performance period, and Dr. Karlheinz Thom of SNSO and Mr. Herbert J. Heppler of the NASA Lewis Research Center for the final portions. The following nine reports (including the present report) comprise the required Final Technical Report under the Contract:

1. Roman, W. C. and J. F. Jaminet: Development of RF Plasma Simulations of In-Reactor Tests of Small Models of the Nuclear Light Bulb Fuel Region. United Aircraft Research Laboratories Report L-910900-12, September 1972.

2. Klein, J. F.: Nuclear Light Bulb Propellant Heating Simulation Using a Tungsten-Particle/Argon Aerosol and Radiation from a DC Arc Surrounded by a Segmented Mirror Cavity. United Aircraft Research Laboratories Report L-910900-13, September 1972.

3. Jaminet, J. F.: Development of a Model and Test Equipment for Cold-Flow Tests at 500 Atm of Small Nuclear Light Bulb Configurations. United Aircraft Research Laboratories Report L-910900-14, September 1972.

4. Kendall, J. S. and R. C. Stoeffler: Conceptual Design Studies and Experiments Related to Cavity Exhaust Systems for Nuclear Light Bulb Configurations. United Aircraft Research Laboratories Report L-910900-15, September 1972.

5. Rodgers, R. J. and T. S. Latham: Analytical Design and Performance Studies of the Nuclear Light Bulb Engine. United Aircraft Research Laboratories Report L-910900-16, September 1972.

6. Latham, T. S. and R. J. Rodgers: Analytical Design and Performance Studies of Nuclear Furnace Tests of Small Nuclear Light Bulb Models. United Aircraft Research Laboratories Report L-910900-17, September 1972.

7. Krascella, N. L.: Spectral Absorption Coefficients of Argon and Silicon and Spectral Reflectivity of Aluminum. United Aircraft Research Laboratories Report L-910904-3, September 1972.

8. Palma, G. E.: Measurements of the UV and VUV Transmission of Optical Materials During High-Energy Electron Irradiation. United Aircraft Research Laboratories Report L-990929-3, September 1972. (Present Report)

9. Kendall, J. S.: Investigation of Gaseous Nuclear Rocket Technology -- Summary Technical Report. United Aircraft Research Laboratories Report L-910905-13, September 1972.

Report L-990929-3

Measurements of the UV and VUV Transmission of Optical Materials During High-Energy Electron Irradiation

TABLE OF CONTENTS

Report L-990929-3

Measurements of the UV and VUV Transmission of Optical Materials During High-Energy Electron Irradiation

SUMMARY

An experimental program was conducted in which the optical transmission of several transparent materials was measured during high-energy electron irradiation. These experiments were conducted at the Space Radiation Effects Laboratory of the NASA Langley Research Center using the Dynamitron electron accelerator as a continuous source of 1.5 MeV electrons and the LINAC electron accelerator as a pulsed source of 5-7 MeV electrons.

The experimental program consisted of three major portions. The first portion, the optical transmission of fused silica, BeO, MgF_2, and LiF was measured at vacuum ultraviolet wavelengths in the range 1550-2000Å during ambient-temperature, 1.5-MeV electron irradiation at ionizing dose rates to 0.5 Mrad/sec. In the second portion of the program, the optical transmission of fused silica and BeO was measured in the range 2000-3000Å during high-dose-rate, elevated-temperature 1.5-MeV electron irradiation. In particular, accurate measurements of the optical transmission were made at ionizing dose rates as high as 10 Mrad/sec. In the final portion of the program, the optical transmission of fused silica and BeO was measured in the wavelength range 2000-3000Å during pulsed 5- and 7-MeV electron irradiation from the LINAC accelerator. The maximum time-averaged ionizing dose rate was limited to 0.75 Mrad/sec due to accelerator limitations.

RESULTS AND CONCLUSIONS

1. Measurements of the optical transmission of single-crystal beryllium oxide in the absence of irradiation indicate that this material has an ultraviolet cutoff of approximately 1250 Å, compared with 1550 Å for Corning 7940 fused silica.

2. Measurements of the optical transmission of single-crystal beryllium oxide during 1.5-MeV electron irradiation indicate that color centers are generated that result in a continuum optical absorption that extends from visible wavelengths and increases towards ultraviolet wavelengths. These measurements yielded the following quantitative results:

(a) The growth of the induced absorption coefficient at a wavelength of 1800 Å during ambient-temperature irradiation consisted of an initial rapid growth rate of 0.25 cm^{-1}/Mrad which decreased after a dose of 10 Mrad to a slower final growth rate of 10^{-3} cm^{-1}/Mrad.

(b) The growth of the induced absorption coefficient at a wavelength of 2200 Å during ambient-temperature irradiation consisted of an initial rapid growth rate of 0.08 cm^{-1}/Mrad which decreased after a dose of 10 Mrad to a slower final growth rate of 2.5×10^{-3} cm^{-1}/Mrad.

(c) The induced absorption coefficient at a wavelength of 2200 Å increased steadily during high-dose-rate (10 Mrad/sec), high-temperature (800°C) irradiation and did not reach a steady state after a total dose of 10^4 Mrad. The final absorption coefficient of 15 cm^{-1} could not be removed by thermal annealing at 800°C, but was removed by thermal annealing at 1000°C.

3. Measurements of the optical transmission of a single-crystal beryllium oxide specimen after ambient-temperature reactor irradiation to a fast neutron dose of $10^{17}/cm^2$ indicated an induced absorption coefficient of 8.1 cm^{-1} at 2200 Å which decreased to 2.8 cm^{-1} at 4000 Å. Thermal annealing at 800°C resulted in a decrease in the induced absorption to 2.15 cm^{-1} at 2200 Å and 1.3 cm^{-1} at 4000 Å.

4. Measurements of the optical transmission of single-crystal beryllium oxide during pulsed LINAC electron irradiation indicated that:

(a) The growth of the induced absorption coefficient at a wavelength of 2200 Å during ambient-temperature 5-MeV irradiation consisted of an initial rapid growth rate of 0.08 cm^{-1}/Mrad and a slower final growth rate of 2.5×10^{-3} cm^{-1}/Mrad.

(b) The corresponding values for the growth rate at an electron energy of

7 MeV are 0.14 cm^{-1}/Mrad and 2 x 10^{-3} cm^{-1}/Mrad.

5. Measurements of the optical transmission of Corning 7940 fused silica at vuv wavelengths during ambient-temperature 1.5-MeV electron irradiation indicate that the growth rate at these wavelengths is an order-of-magnitude lower than at 2150 Å. Both radiation annealing and thermal annealing are effective in removing the resulting vuv absorption.

6. Measurements of the removal of reactor-irradiation-induced absorption at 2150 Å in Corning 7940 fused silica by high-dose-rate 1.5-MeV electron irradiation indicated complete removal of this absorption by irradiation at 5, 7.5, and 10 Mrad/sec.

7. Measurements of the optical transmission of Corning 7940 fused silica during pulsed LINAC electron irradiation at a wavelength of 2150 Å indicated that

(a) The growth rate of the induced absorption coefficient during ambient-temperature irradiation at an electron energy of 5 MeV was 0.012 cm^{-1}/Mrad.

(b) The steady-state induced absorption coefficient due to elevated-temperature, 7-MeV electron irradiation was consistently lower than that due to 1.5-MeV Dynamitron irradiation at the same specimen temperature and average ionizing dose rate.

8. Measurements of the optical transmission of single-crystal specimens of MgF_2 and LiF at a wavelength of 1800 Å during ambient-temperature 1.5-MeV electron irradiation indicated growth rates of 6 x 10^{-4} cm^{-1}/Mrad and 0.087 cm^{-1}/Mrad, respectively.

INTRODUCTION

Background of Previous Studies

The Research Laboratories of United Aircraft Corporation have been conducting an extensive program to determine the effects of nuclear irradiation on the optical transmission of transparent materials under NASA Contracts NASw-768, NASw-847, and SNPC-70, and under Corporate sponsorship. The purpose of this program has been to determine the level of irradiation-induced optical absorption to be expected in the transparent wall of a full-scale nuclear light bulb engine during normal operation. The material studied most extensively throughout these programs has been Corning 7940 fused silica. Fused silica has good optical transmission, good thermal and structural properties, and is relatively easy to fabricate. In addition, irradiation-induced absorption bands at visible wavelengths, which are related to impurities, do not develop appreciably in high-purity grades of fused silica such as Corning 7940. The irradiation-induced absorption bands that have been observed due to exposure of fused silica to nuclear irradiation are centered at the ultraviolet wavelengths of 2150 Å and 1650 Å, with additional structure sometimes observed near 2700 Å (Refs. 1 through 5).

Previous UARL experimental programs on fused silica have consisted of four distinct types of experiments:

1. Post-irradiation optical transmission measurements in which the reactor irradiation simulated the full-scale engine dose (Ref. 6);

2. In-situ optical transmission measurements in a pulsed reactor which simulated the full-scale engine dose rate (Refs. 7 and 8);

3. In-situ optical transmission measurements in a steady-state reactor which simulated the full-scale engine dose (Ref. 9); and

4. In-situ optical transmission measurements in an electron accelerator which simulated the ionizing dose and dose rate of the full-scale engine (Refs. 10 and 11).

These investigations were restricted almost exclusively to the study of Corning 7940 fused silica at wavelengths longer than 2000 Å. It was found that the most prominent absorption band (2150 Å) was generated by ionizing radiation and that the growth rate at a given ionizing dose rate was independent of the type of radiation (i.e. gamma ray, reactor, or electron). Thus, a radiation source with an ionizing dose rate comparable to the full-scale engine (5 Mrad/sec) could provide simulation of the radiation effects expected in a transparent

wall of high-purity fused silica. These high ionizing dose rates were obtained during the FY 1969, FY 1970, and FY 1971 programs using a 1.5-MeV Dynamitron electron accelerator. In particular, accurate measurements of the optical transmission of fused silica were made at ambient and elevated temperatures during 1.5 MeV electron irradiation in the FY 1970 program (Ref. 10). Extensive measurements of the steady-state irradiation-induced absorption coefficient at 2150 Å were made over a wide range of ionizing dose rates (0.02-5 Mrad/sec) and specimen temperatures (100-500°C). It was found that, at constant ionizing dose rate, the induced absorption coefficient decreased with increasing specimen temperature due to the corresponding increase in the thermal annealing rate. However, at constant temperature, the absorption coefficient increased with increasing ionizing dose rate up to a dose rate of 0.4 Mrad/sec. Above this ionizing dose rate, the induced absorption coefficient decreased with further increases in dose rate. This variation of the steady-state induced absorption coefficient with dose rate could be interpreted if it was assumed that the annealing rate increased rapidly with dose rate, a phenomenon that is referred to as "radiation annealing". This interpretation was verified by removing reactor irradiation-induced absorption with 1.5-MeV electron irradiation at temperatures at which the thermal annealing rate is known to be negligible. In addition, measurements of the rate of removal of induced absorption by bleaching with ultraviolet light were made at low light intensities. Extrapolation of these results to the light intensity expected in the full-scale engine indicated that optical bleaching may reduce the level of irradiation-induced absorption by an order of magnitude. Based on these results, the expected additional heat load due to radiation-induced absorption in the transparent wall of the full-scale engine is expected to be negligible for the case of high-purity Corning 7940 fused silica.

High-purity fused silica has an intrinsic ultraviolet cutoff wavelength of approximately 1600 Å, below which it is highly opaque. A transparent material with a lower ultraviolet cutoff could transmit a greater fraction of the radiant energy emitted by the fuel region of the nuclear light bulb engine and could result in a more efficient engine. In particular, a transparent wall material with a significantly lower ultraviolet cutoff would be of interest in a higher performance version of the nuclear light bulb engine having a radiating temperature higher than the reference engine value of 8333°K. Any such candidate material should also have thermal and structural properties comparable to, or better than, those of fused silica; it must also remain relatively transparent during nuclear irradiation. For this reason, experiments were conducted during the FY 1971 program (Ref. 11) in which the optical transmission of several other promising transparent materials was measured during 1.5-MeV electron irradiation. The materials studied were single crystal MgF_2, BaF_2, LiF and BeO, each having ultraviolet cutoff wavelengths near 1200 Å, considerably shorter than that of fused silica. It was found that, of these materials, only single crystal BeO had sufficient resistance to radiation-induced coloration to warrant further experimental study. In single crystal form, this material has an ultraviolet transmission cutoff near 1200 Å, and an extremely high melting point of 2800°C. In addition, the thermal conductivity of beryllium oxide is approximately 2 W/cm-°C at room temperature. This is extremely high for a dielectric material; it is about two orders of magnitude higher than that of fused silica. The thermal conductivity of crystalline BeO is compared with that of ceramic BeO, Corning 7940 fused silica, and copper in Fig. 1 (data from Refs. 12,

13, and 14). The optical transmission measurements made on single crystal beryllium oxide during FY 1971 program were limited to a single specimen of very small dimensions (1 mm x 5 mm x 5mm) and were restricted to wavelengths longer than 2000 Å. The latter restriction was due to experimental difficulties encountered in making in-situ optical transmission measurements at vacuum ultraviolet wavelengths during that program.

Scope of Present Studies

To further assess the effects of electron irradiation on the optical transmission of single crystal beryllium oxide, a set of six single-crystal specimens of adequate dimensions (1 cm x 1 cm x 1 mm) and of good optical quality were obtained from North American Autonetics for the experimental program reported herein (FY 1972). In addition, the difficulties encountered in making in-situ measurements in the vacuum ultraviolet were eliminated by a redesign of the optical system so that it was possible to measure optical transmission of several materials during 1.5-MeV electron irradiation at wavelengths as short as 1500 Å. The materials for these vuv tests included single crystal MgF_2 and LiF, as well as beryllium oxide and fused silica. The measurements were restricted to low dose rates and ambient temperatures to insure an adequate signal-to-noise ratio for the measurements and to avoid the effects of outgassing on the purity of the purge gas.

Accurate measurements of the optical transmission of fused silica and beryllium oxide during 1.5-MeV electron irradiation at wavelengths longer than 2000 Å were made during the present program at ionizing dose rates as high as 10 Mrad/sec. The increase in accuracy over previous measurements was due in part to a more uniform specimen temperature distribution which minimized the effects of refractive index gradients on the transmission measurements.

The validity of the simulation of the nuclear radiation effects on the transparent wall of the nuclear light bulb engine by irradiation with 1.5-MeV electrons from a Dynamitron accelerator has been established with a reasonable degree of assurance for fused silica, but not necessarily for other candidate materials such as beryllium oxide. It is believed that the generation of the defects associated with the irradiation-induced absorption in fused silica is due to ionization of the target atoms rather than the displacement of target atoms from their lattice positions. This result was obtained by a series of experiments involving gamma irradiation, 1.5-MeV electron irradiation, and pulsed and steady-state reactor irradiation. The generation of atomic displacements by neutrons did not appear to contribute to the coloration process and, in fact, the rate of generation of induced absorption was proportional to the ionizing dose rate. An experimental program involving in-situ reactor irradiation measurements of beryllium oxide would not be feasible at this time due to the lack of corner cube specimens of this material. However, information related to the damage mechanism in this material, as well as in fused silica, could

be obtained using an electron irradiation source of variable electron kinetic energy. The energy transferred to target atoms is strongly dependent on the incident electron kinetic energy and is given by (from Ref. 15)

$$T_m = \frac{2147.8}{A} E (E + 1) \qquad (1)$$

where A is the atomic weight of the target material, E is the electron kinetic energy in MeV, and T_m is the maximum energy transfer in eV.

In beryllium oxide ($A_{avg} = 12.5$) for example, T_m increases from 650 eV at E = 1.5 MeV to 19 keV at E = 10 MeV. The latter figure begins to approach the energy transfer due to 1.5-MeV neutron irradiation of approximately 400 keV. Although the Dynamitron electron accelerator energy range is limited to about 1-2 MeV, the pulsed LINAC electron accelerator has an energy range of 3-10 MeV. This accelerator provides a repetitively pulsed 1-cm-diam beam of electrons at average currents up to 6 $\mu A/cm^2$. Thus, average ionizing dose rates close to those obtained with the Dynamitron are available, with the added advantages of variable energy and very high peak dose rates during the pulses. Measurements of the optical transmission of fused silica and beryllium oxide were made during pulsed LINAC irradition in the present program to determine if higher energy electrons were more effective in creating radiation-induced optical absorption in these materials.

The equipment and experimental technique used are discussed in the following section of this report. Next, the important experimental results from the BeO studies, the fused silica studies, and the MgF_2 and LiF studies are presented in separate sections. This is followed by a discussion of the results, with particular consideration of the relative merits of fused silica and single-crystal beryllium oxide as candidate materials for the transparent wall of the nuclear light bulb engine.

DESCRIPTION OF EQUIPMENT AND EXPERIMENTAL TECHNIQUES

The electron irradiation experiments were conducted during two separate periods at the Space Radiation Effects Laboratory of the NASA Langley Research Center in Hampton, Virginia.

The first set of experiments was conducted during the period of March 6-17, 1972 and utilized the Dynamitron electron accelerator as a radiation source at an electron energy of 1.5 MeV. Data pertaining to the optical transmission of fused silica, single crystal beryllium oxide (BeO), magnesium fluoride (MgF_2), and lithium fluoride (LiF) during electron irradiation were obtained at wavelengths as short as 1500 Å.

The second set of experiments was conducted during the week of May 22-27, 1972 and utilized the pulsed LINAC electron accelerator as a radiation source. This accelerator provided average ionizing dose rates up to 0.75 Mrad/sec at energies of 5 and 7 MeV in a repetitively pulsed mode of operation. The pulse width and repetition rate were varied over the range 100 to 500 nsec and 60 to 360 pps, respectively. In the LINAC experiments, the optical transmission of fused silica and single-crystal BeO specimens was measured at wavelengths in the range 2000 to 3000 Å.

Vacuum Ultraviolet Experimental Arrangement

Figure 2 is a combined optical and electronic schematic that illustrates the important experimental components with their respective locations. This system was modified from the system used in previous tests to extend the wavelength capability to 1500 Å. The optical path from the hydrogen lamp to the monochromator entrance slit was sealed in a plexiglass chamber which was purged with high purity (99.995 percent) nitrogen to minimize atmospheric absorption at vuv wavelengths. A modified sample chamber was used. It was sealed with a polyvinyl-fluoride window which could transmit the electron beam with little energy loss. This sample chamber did not include a furnace assembly. Although the nitrogen purge system was successful in reducing the atmospheric absorption to an acceptable level, the signal strength was still an order of magnitude lower at 1500 Å than at 2000 Å . This was due to the limitations imposed by the light source intensity and the photomultiplier spectral response. This resulted in a lower signal-to-noise ratio at vuv wavelengths which limited the maximum allowable ionizing dose rate to 0.50 Mrad/sec. All irradiations in which vuv measurements were made were performed at ambient temperature to eliminate additional absorption due to outgassing of furnace components at elevated temperatures.

High Dose Rate Experimental System and Specimen Configuration

The experimental arrangement for the high-dose-rate Dynamitron irradiations was similar to that shown in Fig. 2, except that the purge system was removed since optical transmission measurements were not attempted at vuv wavelengths. The furnace assembly and specimen holder from previous programs was also employed for operation at elevated specimen temperatures.

The specimen configuration was slightly different from that used in previous high-dose-rate experiments. In previous experiments (Refs. 10 and 11), the specimens were approximately 2 cm in cross-section, so that the 1-cm-diam electron beam irradiated only a portion of the specimen. This resulted in a non-uniform temperature distribution which caused a lensing effect due to the corresponding gradient in the refractive index. This lensing effect sometimes resulted in a decrease in signal that was not due to actual optical absorption. It was found that a smaller specimen cross-section of 1 cm x 1 cm resulted in a more uniform temperature distribution and the elimination of any anomalous loss of signal.

The average temperature across the area of the light beam is somewhat higher than the temperature measured at the edge due to the finite temperature gradient in the specimen. For a uniform electron beam energy deposition, the radial temperature distribution is, according to theory, parabolic with a maximum at the center of the beam. The average temperature for this case is greater than the measured temperature by an amount ΔT given by

$$\Delta T = \frac{\dot{Q} r_\ell^2}{8k} \qquad (2)$$

where Q = electron beam heat deposition (W/cm^3), r_ℓ = light beam radius = 0.3 cm, and k = thermal conductivity = 0.02 W/cm-°C. The effect of this temperature difference on interpretation of the data is discussed later.

LINAC Irradiation Experimental Arrangement

The optical and electronic system was similar to that used in the high-dose-rate Dynamitron experiments, and in fact the LINAC and Dynamitron accelerator target areas are identical. However, a considerable amount of additional lead shielding was required due to the higher energy of the irradiations. The maximum time-averaged ionizing dose rate for these experiments was limited to 0.75 Mrad/sec due to difficulties with the LINAC accelerator vacuum system.

EXPERIMENTAL RESULTS

The experimental results are usually expressed as induced absorption coefficients which are calculated from the chart recorder transmission data using the following equation:

$$\alpha(\lambda) = \frac{1}{\ell} \ln \left[\frac{I(\lambda, T, \dot{D}, t)}{I_o(\lambda)}\right] \qquad (3)$$

where $\alpha(\lambda)$ = irradiation-induced absorption coefficient at the wavelength λ (cm^{-1}), ℓ = optical path length through specimen (cm), $I_o(\lambda)$ = chart recorder amplitude prior to irradiation, and $I(\lambda, T, \dot{D}, t)$ = chart recorder amplitude at a time t after turn-on of electron beam.

Beryllium Oxide Studies

A total of six single-crystal beryllium oxide specimens were used. As data on the optical transmission of single-crystal beryllium oxide was lacking at the onset of this program, an initial experiment was performed in cooperation with Prof. C. Peterson of the University of Connecticut in which the intrinsic optical transmission of BeO was measured over the wavelength interval 1000-2800 Å. The results are presented in Fig. 3, in which a comparison is made of the optical transmission of BeO and Corning 7940 fused silica. The beryllium oxide specimen is seen to have measurable transmission down to a wavelength of 1250 Å, whereas the fused silica becomes essentially opaque at a longer wavelength of 1550 Å. Insufficient information was available on the indexed refraction of either BeO or SiO_2 at these wavelengths to separate absorption from reflection losses. After this preliminary characterization of the optical transmission of single-crystal BeO, the series of irradiation experiments described below was conducted in which the effects of electron and reactor irradiation on optical transmission were investigated.

1.5-MeV Electron Irradiation of BeO

The results of measurements of the optical transmission of single-crystal beryllium oxide specimen BeO-1 at a vuv wavelength of 1800 Å during continuous ambient-temperature 1.5-MeV electron irradiation are shown in Fig. 4. When the Dynamitron accelerator is turned on at an ionizing dose rate of 0.1 Mrad/sec, the induced absorption coefficient increases initially at a rate of 0.25 cm^{-1}/Mrad. This initial growth rate saturates when the induced absorption coefficient reaches 2.5 cm^{-1}, and a much slower growth rate of approximately 10^{-3} cm^{-1}/Mrad is observed for the remainder of the irradiation. This is a preliminary indication that the irradiation-induced optical absorption in BeO is due to two types of color centers

with significantly different rates of generation. The vuv absorption spectrum of specimen BeO-1 measured after this irradiation is shown in Fig. 5, which indicates a peak at a wavelength of 1650 Å with a decrease in absorption towards longer wavelengths.

The results of measurements of the growth of the induced absorption coefficient at 2200 Å in specimen BeO-2 during ambient-temperature 1.5-MeV electron irradiation are shown in Fig. 6. The growth curve is similar in shape to that measured at a wavelength of 1800 Å (see Fig. 4). As a comparison, the induced absorption coefficient at an ionizing dose of 300 Mrad was 2.5 cm^{-1} at 1800 Å (Fig. 4) and 1.5 cm^{-1} at 2200 Å (Fig. 6). This indicates that the absorption is decreasing with increasing wavelength, in agreement with the spectrum shown in Fig. 5.

The variation with time of the induced absorption coefficient at 2200 Å in specimen BeO-3 during high-dose-rate, elevated-temperature 1.5-MeV electron irradiation is illustrated in Fig. 7. This experiment was conducted at an ionizing dose rate of 10 Mrad/sec and an initial specimen temperature of 200°C provided by the furnace. At the onset of irradiation, the induced absorption coefficient increases rapidly, reaching a value of approximately 2 cm^{-1} at an elapsed time of 10 sec. As the irradiation continues, the absorption decreases almost to zero at an elapsed time of 100 sec and then begins to gradually increase. This gradual increase continues even at elevated temperatures and is apparently accelerated as the temperature is raised from 600 to 800°C. The electron beam was shut off at an elapsed time of 950 sec and a total dose of 9500 Mrad. At this condition, the absorption coefficient had reached 15 cm^{-1} at 2200 Å. The absorption spectrum of specimen BeO-3 which was measured immediately after this irradiation is shown in Fig. 8. This spectrum is consistent with the previous results in that the absorption is decreasing towards longer wavelengths. After this experiment, specimen BeO-3 was maintained at a temperature of 800°C for a period of 60 min to investigate the effects of thermal annealing on the irradiation-induced absorption. It was found that no measurable decrease in the absorption spectrum resulted from this annealing treatment. However, it might be expected that the annealing temperature of BeO would be higher than that for SiO_2 because of its higher melting point.

Reactor Irradiation of BeO

Specimen BeO-4 was reactor-irradiated to a fast neutron dose of $10^{17}/cm^2$ at the Union Carbide Research Center, Tuxedo, N. Y. The upper curve of Fig. 9 shows the absorption spectrum due to this irradiation over the wavelength interval 2000-4000 Å. The spectral shape is similar to that resulting from 1.5-MeV electron irradiation as shown in Fig. 8. When the specimen was given the thermal annealing treatment shown in Fig. 10, the induced absorption coefficient was observed to decrease to a final value that could not be removed at a temperature of 800°C. The lower curve of Fig. 9 shows the absorption spectrum that remained after this thermal annealing treatment.

Pulsed LINAC Irradiation of BeO

The optical transmission of specimens BeO-5 and BeO-6 was measured during pulsed LINAC electron irradiation at energies of 7 and 5 MeV, respectively. The irradiations were conducted at ambient temperature and at the same wavelength (2200 Å) and average dose rate (0.07 Mrad/sec) employed in the 1.5-MeV Dynamitron irradiation of specimen BeO-2 shown in Fig. 6. The results of these three irradiations have been used to compare the variation of the growth of the induced absorption coefficient with electron energy in Fig. 11. Examination of Fig. 11 indicates that the growth curves at 1.5 and 5 MeV are almost identical, while the growth curve for 7 MeV differs from these only in the initial slope, and the magnitude of the absorption generated during the initial period.

Fused Silica Studies

A total of eleven Corning 7940 fused silica specimens were investigated during the experimental program. Of these, four were used to investigate the growth and spectral shape of radiation-induced absorption at vuv wavelengths due to 1.5-MeV electron irradiation. Three reactor-irradiated specimens were employed in further studies of radiation annealing by high-dose-rate electron irradiation. In addition, four specimens were used in pulsed LINAC electron irradiation experiments, in which a comparison was made between pulsed 5- and 7-MeV irradiation and continuous 1.5-MeV irradiation.

1.5-MeV Electron Irradiation of SiO_2 - VUV Studies

The results of the measurements of the growth of the induced absorption coefficient at a wavelength of 1900 Å during ambient-temperature 1.5-MeV electron irradiation of specimen SV-1 are shown in Fig. 12. The growth curve is approximately linear with a slope of 0.0036 cm^{-1}/Mrad. This value is approximately one order of magnitude lower than the slope of 0.05 cm^{-1}/Mrad measured at 2150 Å in previous programs(Refs.10 and 11). The vuv absorption spectrum of specimen SV-1 which was measured immediately after this irradiation is shown as the upper curve in Fig. 13. The spectrum has some structure but does not have any identifiable peaks. Specimen SV-1 was then irradiated at a dose rate of 5 Mrad/sec and a specimen temperature of 300°C for an elapsed time of 60 sec to investigate the effectiveness of radiation annealing in removing irradiation-induced absorption at vuv wavelengths. The vuv absorption spectrum of specimen SV-1 that was measured immediately after the radiation annealing treatment is shown as the lower curve in Fig. 13. It can be seen that almost complete removal of the vuv absorption has resulted from radiation annealing.

In a similar experiment, specimen SV-2 was irradiated at ambient temperature to an ionizing dose of 1160 Mrad with 1.5-MeV electron irradiation. The results of measurement of the growth of the induced absorption coefficient at 1800 Å are

presented in Fig. 14. The growth curve is again approximately linear with a slope of 0.003 cm^{-1}/Mrad. The resulting absorption spectrum is shown as the solid curve in Fig. 15. The dashed curve in Fig. 15 represents the absorption spectrum after subsequent optical bleaching with a BH-6 mercury arc lamp for a period of 60 min. Apparently, the ultraviolet output of this lamp, which has little intensity at wavelengths shorter than 2000 Å, is ineffective in removing vuv induced optical absorption.

Specimen SV-3 was irradiated at ambient temperature to an ionizing dose of 1360 Mrad at which the resulting induced absorption coefficient at 1650 Å was 2.5 cm^{-1}. The corresponding growth curve is shown in Fig. 16. The specimen was then thermally annealed at 700°C for 60 min; the absorption spectra before and after thermal annealing are shown in Fig. 17 for specimen SV-3. The data indicates that thermal annealing results in almost complete removal of vuv induced absorption in Corning 7940 fused silica.

An experiment was also performed in order to investigate the vuv absorption spectrum in fused silica due to reactor irradiation. Specimen SVN-1 was reactor irradiated at ambient temperature to a fast neutron dose of $10^{17}/cm^2$ in the Union Carbide Research Reactor. The absorption spectra due to this irradiation are illustrated in Fig. 18 before and after a thermal annealing treatment at 700°C for 60 min. An examination of Fig. 18 indicates that the vuv absorption spectrum due to reactor irradiation does not exhibit any pronounced peaks and that thermal annealing at 700°C is effective in removing this absorption.

1.5-MeV Electron Irradiation of SiO_2 - Radiation Annealing Studies

Several high-dose-rate irradiations involving radiation annealing of reactor-irradiated fused silica specimens were conducted during the experimental program in order to conclusively demonstrate this effect. It was found that thermally induced refractive index effects could be minimized by using specimens whose dimensions were comparable to that of the electron beam cross section, i.e. 1 cm x 1 cm. Results of the radiation annealing of reactor-irradiated specimen SCN-1 by 1.5-MeV electron irradiation at an ionizing dose rate of 5 Mrad/sec and a final temperature of 260°C are shown in Fig. 19. An examination of Fig. 19 indicates that the initial absorption coefficient of 15.5 cm^{-1} due to a reactor fast neutron dose of $10^{17}/cm^2$ is completely removed in approximately 200 sec by this high-dose-rate irradiation. Similar results for specimens SCN-2 and SCN-3 are shown in Fig. 20 and 21 for which the ionizing dose rates were 7.5 and 10 Mrad/sec respectively. Note that the rate of removal of absorption increases with the ionizing dose rate.

Pulsed LINAC Irradiation of SiO_2

A set of experiments was conducted to investigate the effects of repetitively pulsed electron irradiation from a LINAC electron accelerator on the optical transmission of Corning 7940 fused silica. The pulse repetition rate and pulse duration were varied from 60-240 pps and 0.175-0.5 μsec, respectively. The maximum ionizing dose rate was limited to 0.75 Mrad/sec due to difficulties with the accelerator vacuum system.

The results of the growth of the induced absorption coefficient at 2150 Å for specimen SL-1 during ambient-temperature irradiation at an average ionizing dose rate of 0.1 Mrad/sec and an electron kinetic energy of 5 MeV are illustrated in Fig. 22. The growth curve is linear, as observed in Dynamitron irradiation; however, the magnitude of the slope is 0.012 cm^{-1}/Mrad, which is considerably less than the value of 0.05 cm^{-1}/Mrad measured in previous Dynamitron experiments (Refs. 10 and 11). This slower growth rate may be due to radiation annealing occurring at the high peak dose rate ($\sim 10^5$ Mrad/sec) during the pulse. In any case there does not appear to be any increase in damage due to the higher electron energy of 5 MeV.

The results of the measurement of the induced absorption coefficient at 2150 Å for specimens SL-2, SL-3, and SL-4 during 7-MeV pulsed-electron irradiation at elevated temperatures are shown in Figs. 23, 24, and 25. In these experiments the pulse width was held constant at 0.5 μ sec and the average ionizing dose rate was varied from 0.25-0.75 Mrad/sec by varying the pulse repetition rate from 120-360 pps. The specimen temperature was controlled by the furnace as the heating due to the electron beam was not significant. Referring to Fig. 23, we see that, at an average ionizing dose rate of 0.25 Mrad/sec and a specimen temperature of 200°C, the equilibrium absorption coefficient was 2.1 cm^{-1}. Similarly, at an ionizing dose rate of 0.25 Mrad/sec and a specimen temperature of 340°C, the absorption coefficient was only 0.2 cm^{-1}. The corresponding values measured during 1.5-MeV Dynamitron irradiation as reported in Refs. 10 and 11 were 4.2 cm^{-1} and 2 cm^{-1}. The data shown in Figs. 24 and 25 at ionizing dose rates of 0.50 and 0.75 Mrad/sec are also consistently lower in value than the corresponding values measured during Dynamitron irradiation. It thus appears that pulsed electron irradiation, despite higher electron energy, is less effective than continuous electron irradiation in generating color centers. As mentioned previously, this may be due to radiation annealing during the high-peak-dose-rate portion of the pulses.

1.5-MeV Electron Irradiation of MgF_2 and LiF - VUV Studies

In addition to the extensive experiments on BeO and fused silica, measurements were made of the optical transmission of single crystal MgF_2 and LiF at vuv wavelengths during 1.5-MeV electron irradiation. Although these materials are not of primary interest for nuclear light bulb applications due to their poor structural and thermal properties, these data were obtained to compliment previous data taken at longer wavelengths (Ref. 11).

The growth of the induced absorption coefficient in MgF_2 at 1800 Å during ambient-temperature 1.5-MeV electron irradiation is shown in Fig. 26. The observed growth rate at this wavelength of 6×10^{-4} cm^{-1}/Mrad is extremely slow, indicating a very high radiation resistance at vuv wavelengths for this material. However, as the spectral absorption curve of Fig. 27 indicates, the induced absorption coefficient increases rapidly at longer wavelengths, in agreement with the results of Ref. 11.

The results of the growth of the induced absorption coefficient at 1800 Å during 1.5-MeV electron irradiation for single crystal LiF, as shown in Fig. 28, indicates a much higher growth rate of 0.1 cm^{-1}/Mrad for this material. The measured vuv absorption spectrum is shown in Fig. 29, and indicates an absorption band centered at approximately 1750 Å.

DISCUSSION OF RESULTS

The results of measurements of the optical transmission of single crystal beryllium oxide during ambient-temperature electron irradiation and following reactor irradiation indicates that such irradiations generate color centers in this material with a broadband optical absorption spectrum (see Figs. 5, 8, and 9). The measurements made during electron irradiation indicate that the observed coloration is due to two different types of color centers. One type of center has a rapid growth rate evidenced by an initial rapid rise in induced absorption of 0.08-0.25 cm^{-1}/Mrad (Figs. 4, 6, 11) which saturates at an ionizing dose of approximately 10 Mrad. Superimposed on this rapid growth rate is a much slower growth rate, on the order of 10^{-3} cm^{-1}/Mrad, which is apparently due to a second type of color center which requires a much higher degree of damage for its generation. Measurements of the thermal annealing rate (Fig. 10) indicate that the color centers responsible for the initial rapid growth can be annealed at temperatures above 200°C. However, the color centers responsible for the final slow growth rate could not be thermally annealed at temperatures as high as 800°C. This interpretation is consistent with the variation of the induced absorption coefficient during high-dose-rate irradiation as shown in Fig. 7. There is an initial rapid increase which saturates and then decays rapidly as the temperature exceeds 200°C. This initial behavior is apparently due to the generation and subsequent thermal annealing of the short-lived color centers. Superimposed on this initial transient is a steady growth which results in an induced absorption coefficient of 15 cm^{-1} after a total ionizing dose of 9500 Mrad. This corresponds to an average growth rate of 1.6×10^{-3} cm^{-1}/Mrad, comparable to that measured at ambient temperature and low dose rate (see Fig. 6), which is apparently unaffected by the high temperature (800°C) of this irradiation. This behavior is consistent with the model of a color center that does not anneal at temperatures below 800°C.

The results of the experiments on single crystal beryllium oxide indicate that this material would not be as suitable as fused silica for use in the transparent wall of the nuclear light bulb engine unless the wall temperatures are kept high. The data indicate that, at the nominal ionizing dose rate of the full-scale engine of 5 Mrad/sec and a wall temperature of 800°C or lower, broadband optical absorption on the order of 5 cm^{-1} would be generated during the 1000-sec running time.

After the irradiation experiments were concluded, a heavily irradiated BeO specimen was annealed at 1000°C for 60 min in a higher temperature furnace. This treatment resulted in almost complete removal of the irradiation-induced absorption. It thus appears that the long-lived color centers in BeO can be annealed at temperatures of 1000°C. This very high annealing temperature is consistent with the high melting point (2800°C) of single crystal BeO, since both annealing of defects and melting are functions of lattice mobility. Since there is more heat sink capacity in a nuclear light bulb engine at high temperatures than at low temperatures, and since BeO retains its structural strength to a higher temperature than does S_iO_2, the higher temperatures required for a BeO wall are actually an advantage.

The results of the optical transmission measurements on Corning 7940 fused silica made during this program are consistent with those presented in Refs. 10 and 11, and indicate that this material is highly suitable as transparent wall material for the nuclear light bulb engine. Some new results of the growth of the irradiation-induced absorption at vuv wavelengths (1500-1900 A) during 1.5-MeV electron irradiation indicate that the growth rate is an order of magnitude slower than at 2150 Å (see Figs. 12 through 18). In addition, this vuv absorption is readily removed by either radiation annealing or thermal annealing.

With regard to radiation annealing in fused silica, accurate data on the removal of reactor-irradiation induced absorption by high-dose-rate 1.5-MeV electron irradiation was obtained during the present program (see Figs. 19, 20, and 21). Several high-dose-rate irradiations involving radiation annealing of reactor-irradiated fused silica specimens were conducted. It was found that at a dose rate of 10 Mrad/sec and a measured specimen temperature of 410°C, complete removal of initial reactor-induced absorption occurred in 25 sec from turn-on of the electron beam. At 5 Mrad/sec and 260°C, transparency was restored in about 200 sec. These temperatures were measured at the edge of the light beam approximately 3 mm from the center of both the electron and light beam axes as shown in Fig. 30.

The important question arises as to whether the actual average temperature in the high-dose-rate experiments was significantly higher than the measured temperature. If this were the case, the rapid removal of absorption at high dose rates could be attributed to purely thermal annealing rather than to a radiation annealing process. However, at an ionizing dose rate of 5 Mrad/sec and a measured temperature of 260°C, the heat deposition rate of 110 W/cm^3 results in $\Delta T = 60°C$ and an average estimated temperature of 320°C. The thermal annealing rate at 320°C is not significantly greater than that at 260°C and is not rapid enough in either case to account for the very low levels of absorption measured at these conditions.

Measurements were also made during the present program of the effects of pulsed 5-and 7-MeV electron irradiation on the optical transmission of single crystal BeO and Corning 7940 fused silica. The results for BeO indicate an increase in the initial growth rate at 7 MeV as compared with those measured at 5 and 1.5 MeV (see Fig. 11). However, the final growth rate due to long-lived defects was observed to be approximately independent of electron kinetic energy in this material. In the case of fused silica, the measured growth rates and steady state levels of induced absorption were actually lower during pulsed 5-and 7-MeV irradiation than the corresponding values measured during continuous 1.5-MeV irradiation (see Figs. 22 through 25). This discrepancy is believed to be due to removal of absorption by radiation annealing during the electron pulse where the instantaneous ionizing dose rate is extremely high ($\approx 10^5$ Mrad/sec).

The results of this experimental program indicate that single crystal beryllium oxide would only be suitable for use in the transparent wall of the nuclear light bulb engine at wall temperatures higher than 800°C. The actual level of irradiation-induced optical absorption at higher temperatures was not determined in the present program and would require further experimentation. The results of measurements of the optical transmission of fused silica during irradiation in this and previous programs indicate that this material would remain highly transparent down to a wavelength of about 1650 Å at high ionizing dose rates (5-10 Mrad/sec) and moderate temperatures (≥ 300°C).

REFERENCES

1. Compton, W. D. and G. W. Arnold, Jr.: Radiation Effects in Fused Silica and α-Al_2O_3. Discussions Faraday Soc., vol. 31, 1961, p. 130.

2. Nelson, C. W. and J. H. Crawford, Jr.: Optical Absorption in Irradiated Quartz and Fused Silica. J. Phys. Chem. Sol., vol. 13, 1960, p. 296.

3. Nelson, C. M. and R. A. Weeks: Trapped Electrons in Irradiated Quartz and Silica. J. Am. Ceram. Soc., vol. 43, 1960, p. 396.

4. Nelson, C. M. and R. A. Weeks: Vacuum-Ultraviolet Absorption Studies of Irradiated Silica and Quartz. J. Appl. Phys., vol. 32, 1961, p. 883.

5. Levy, P. W.: Reactor and Gamma-Ray Induced Coloring of Corning Fused Silica. J. Phys. Chem. Sol., vol. 13, 1960, p. 287.

6. Gagosz, R. M., F. C. Douglas and M. A. DeCrescente: Optical Absorption in Transparent Materials Following High-Temperature Reactor Irradiation. United Aircraft Research Laboratories Report F-910485-2, prepared under Contract NASw-847, September 1967. Also issued as NASA CR-1032.

7. Gagosz, R. M., J. P. Waters, F. C. Douglas and M. A. DeCrescente: Optical Absorption in Fused Silica During Triga Reactor Pulse Irradiations. United Aircraft Research Laboratories Report F-910485-1, prepared under Contract NASw-847, September 1967. Also issued as NASA CR-1031.

8. Gagosz, R. M. and J. P. Waters: Optical Absorption and Fluorescence in Fused Silica During Triga Pulse Irradiations. United Aircraft Research Laboratories Report G-910485-3, prepared under Contract NASw-847, April 1968. Also issued as NASA CR-1191.

9. Palma, G. E. and R. G. Gagosz: Optical Absorption in Fused Silica During Irradiation at High Temperature. United Aircraft Research Laboratories Report H-930709-1, prepared under Contract NASw-847, October 1969.

10. Palma, G. E. and R. M. Gagosz: Optical Absorption in Transparent Materials During 1.5 MeV Electron Irradiation. United Aircraft Research Laboratories Report J-990929-1, prepared under Contract SNPC-70, October 1970.

11. Palma, G. E. and R. M. Gagosz: Effect of 1.5 MeV Irradiation on the Transmission of Optical Materials. United Aircraft Research Laboratories Report K-990929-2, prepared under Contract SNPC-70, September 1971.

12. Slach, G. A. and S. B. Austerman: Thermal Conductivity of BeO Single Crystals. J. Appl. Phys., vol. 42, no. 12, November 1971.

13. Anon: Properties of Corning 7940 Fused Silica. Corning Glass Works, January 1965.

14. Anon: Handbook of Chemistry and Physics. Chemical Rubber Publishing Company.

15. Corbett, J. W.: Electron Radiation Damage in Semiconductors and Metals. Academic Press, New York and London, 1966, pp. 30-36.

LIST OF SYMBOLS

A	Atomic weight, dimensionless
D	Ionizing dose, Mrad
$\dot{D}$	Ionizing dose rate, Mrad/sec
E	Electron kinetic energy, MeV
$I_o(\lambda)$	Chart recorder amplitude prior to irradiation, dimensionless
$I(\lambda,T,\dot{D},t)$	Chart recorder amplitude during irradiation, dimensionless
k	Thermal conductivity, W/cm-°C
ℓ	Optical path length, cm
$\dot{Q}$	Electron beam heat deposition, W/cm^3
r_e	Electron beam radius, cm
r_ℓ	Light beam radius, cm
t	Elapsed time, sec
T	Specimen temperature, °C
T_m	Maximum energy transfer, eV
$\alpha(\lambda)$	Induced absorption coefficient at a wavelength λ, cm^{-1}
λ	Wavelength, Å

FIG. 1

COMPARISON OF RECENT MEASUREMENTS OF SINGLE CRYSTAL BeO, THERMAL CONDUCTIVITY WITH CONDUCTIVITIES OF CERAMIC BeO, FUSED SILICA AND COPPER

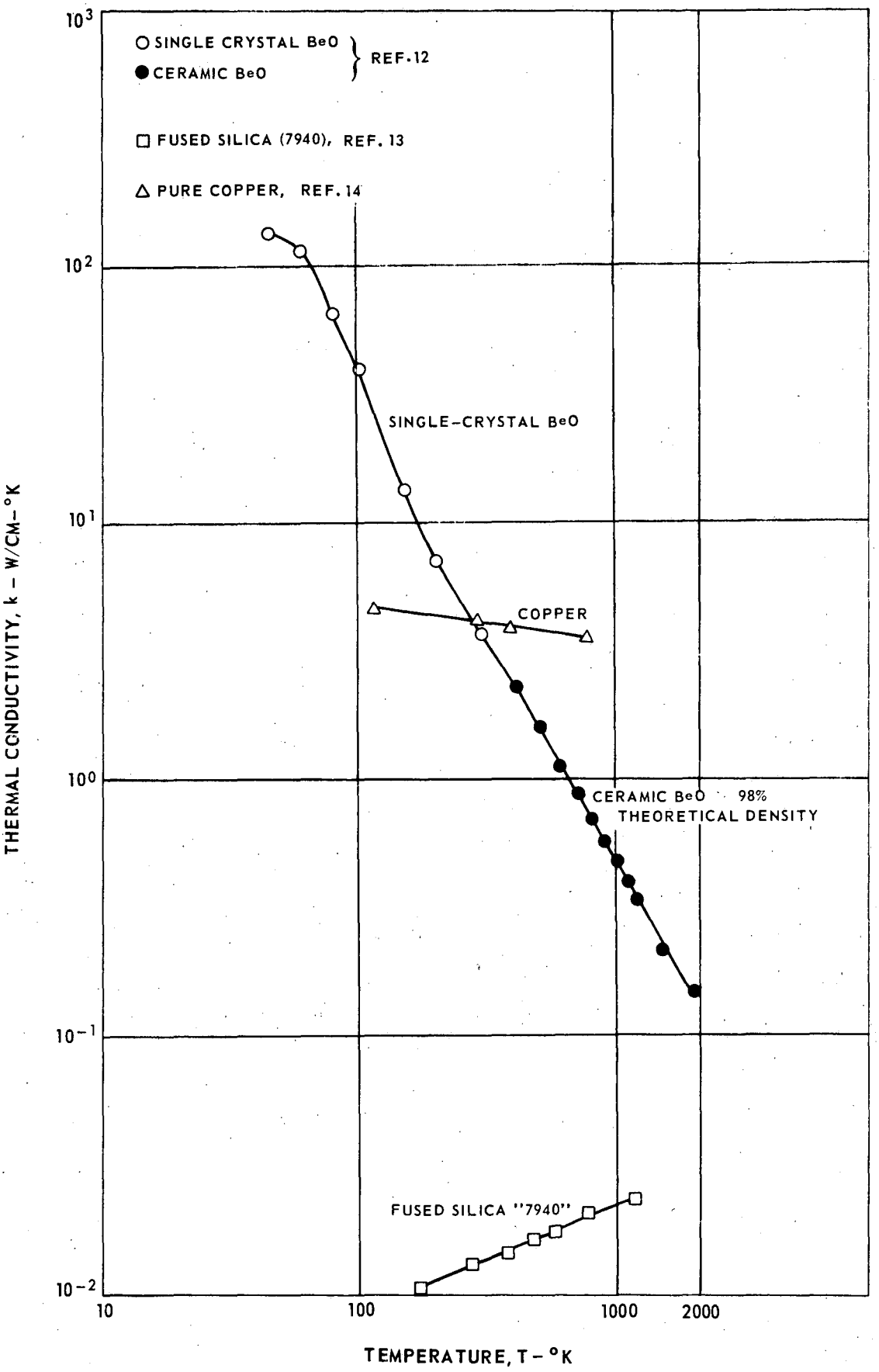

L-990929-3

FIG. 2

ELECTRICAL AND OPTICAL SCHEMATIC FOR VUV ELECTRON IRRADIATION EXPERIMENTS

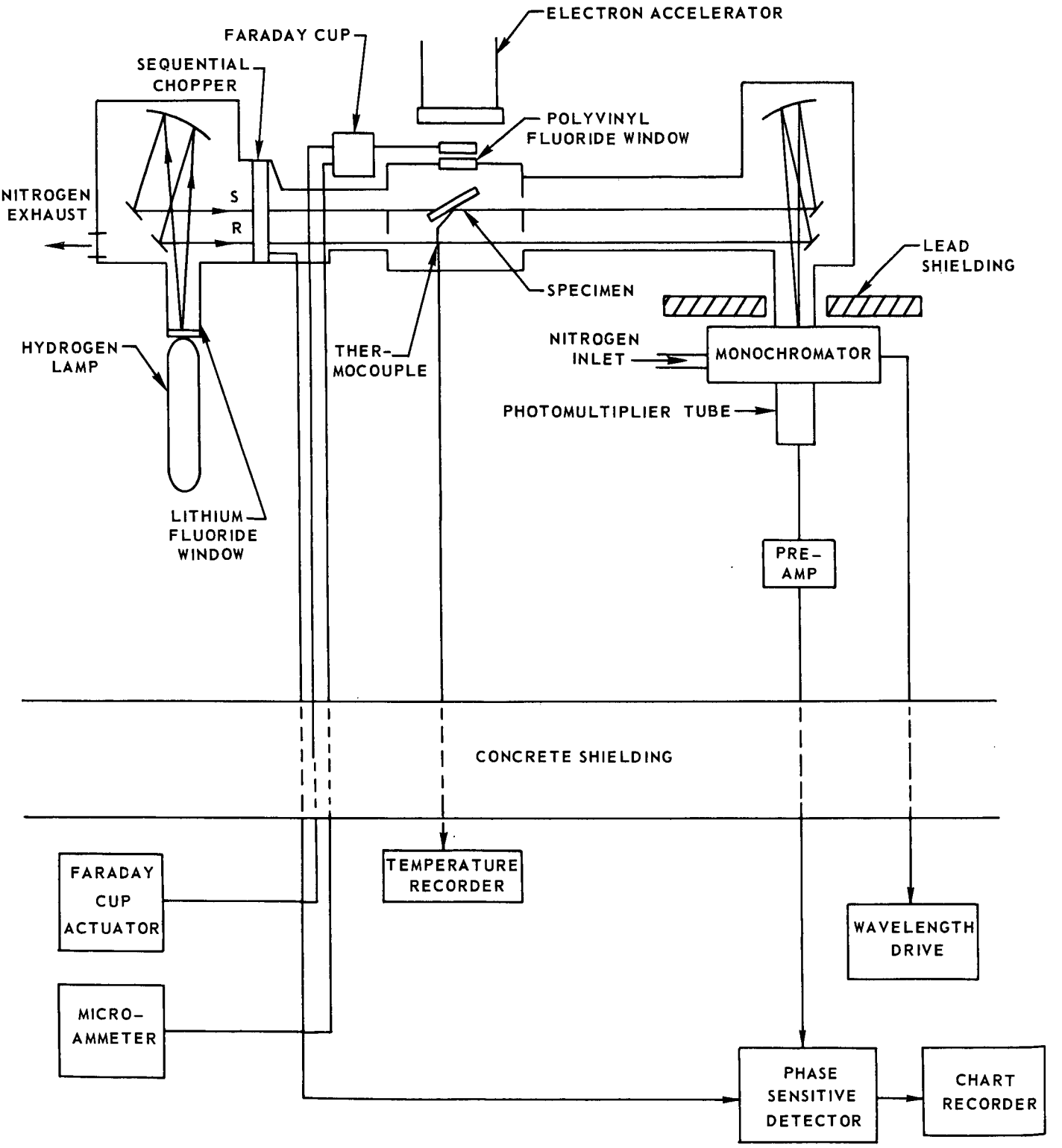

FIG. 3

COMPARISON OF VUV OPTICAL TRANSMISSION OF CORNING 7940 FUSED SILICA AND SINGLE CRYSTAL BERYLLIUM OXIDE

○ 1 MM SINGLE CRYSTAL BeO – DATA OF C. PETERSON, U. CONN.

△ 1.5 MM CORNING 7940 FUSED SILICA – UARL DATA

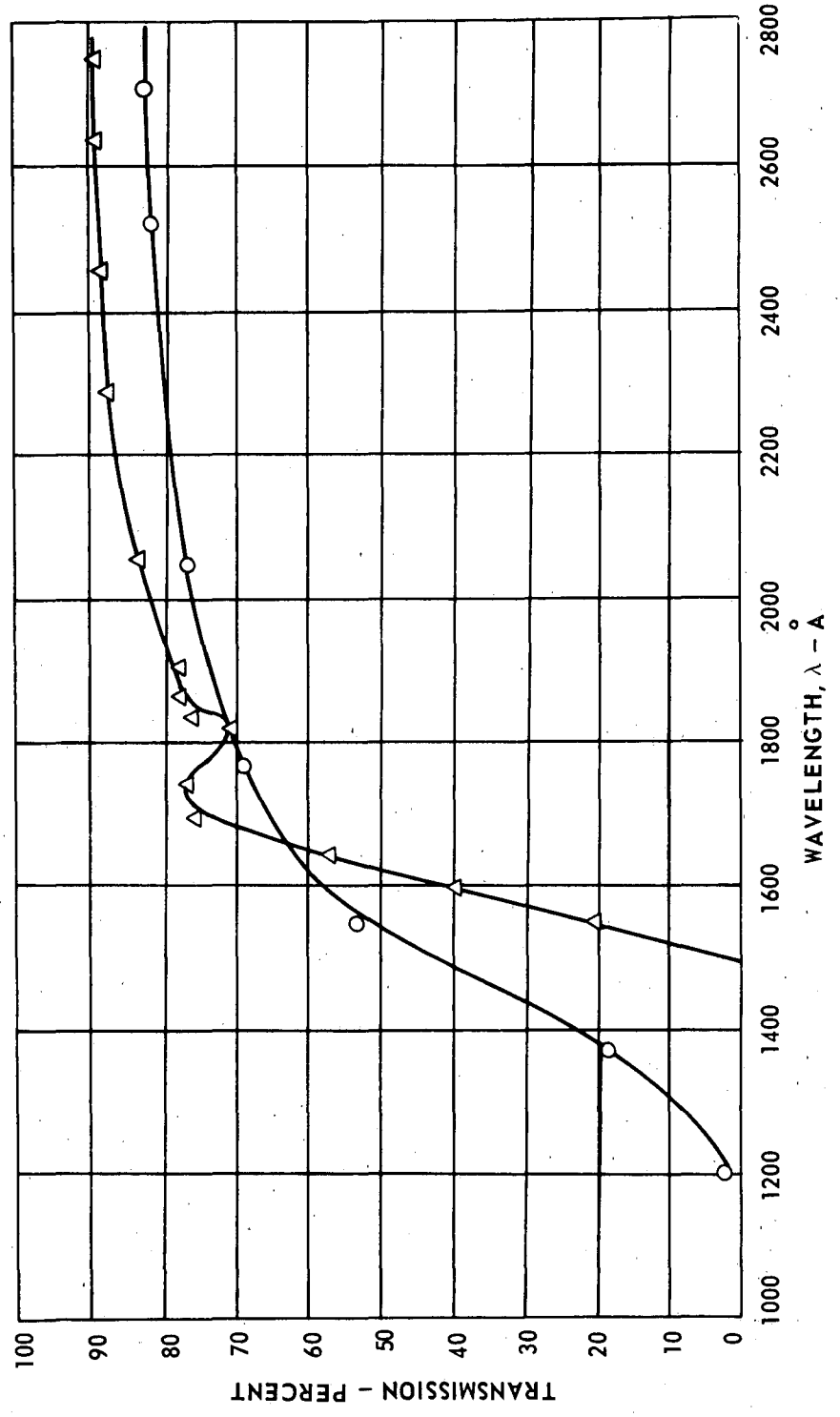

L-990929-3

GROWTH OF INDUCED ABSORPTION FOR BERYLLIUM OXIDE SPECIMEN BEO-1 DURING 1.5-MEV ELECTRON IRRADIATION

$\lambda = 1800$ Å

$\dot{D} = 0.1$ MRAD/SEC

$T = 40°C$

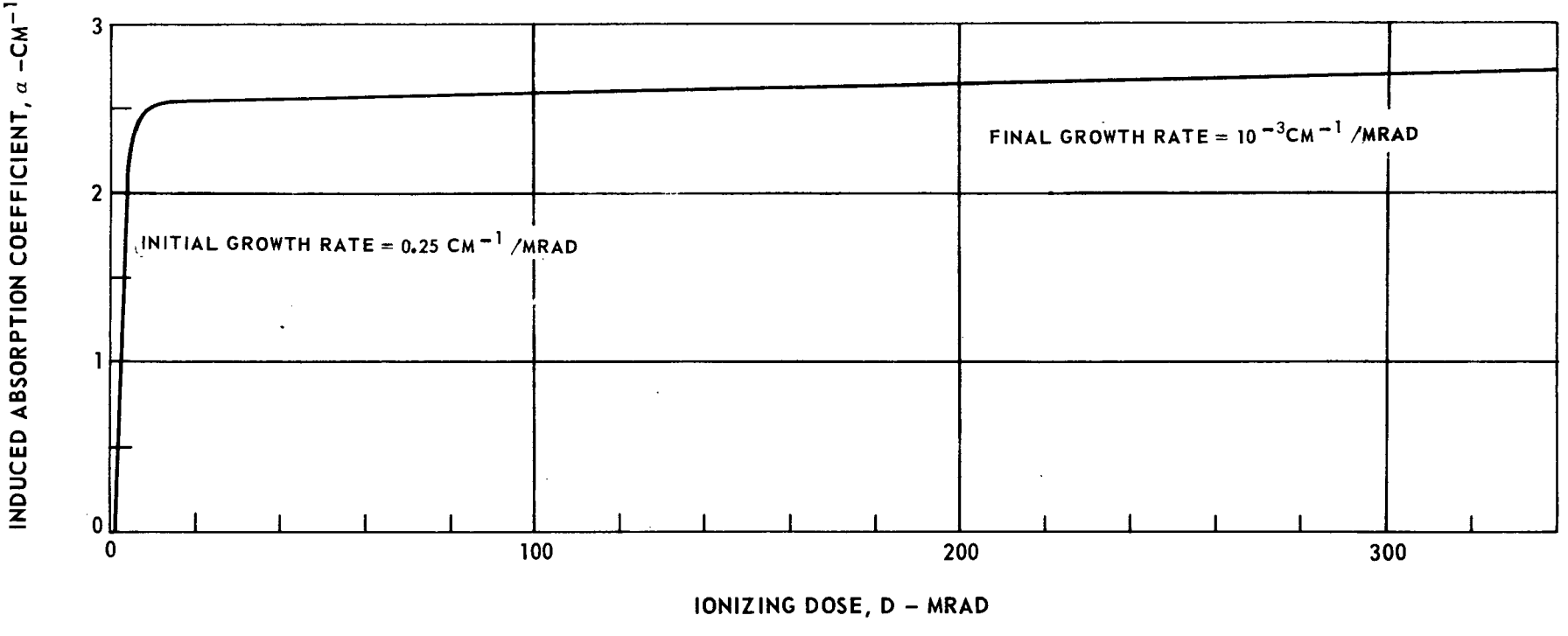

FIG. 4

VACUUM UV ABSORPTION SPECTRUM OF BERYLLIUM OXIDE SPECIMEN BEO-1 FOLLOWING 1.5-MEV ELECTRON IRRADIATION

IONIZING DOSE D = 310 MRAD

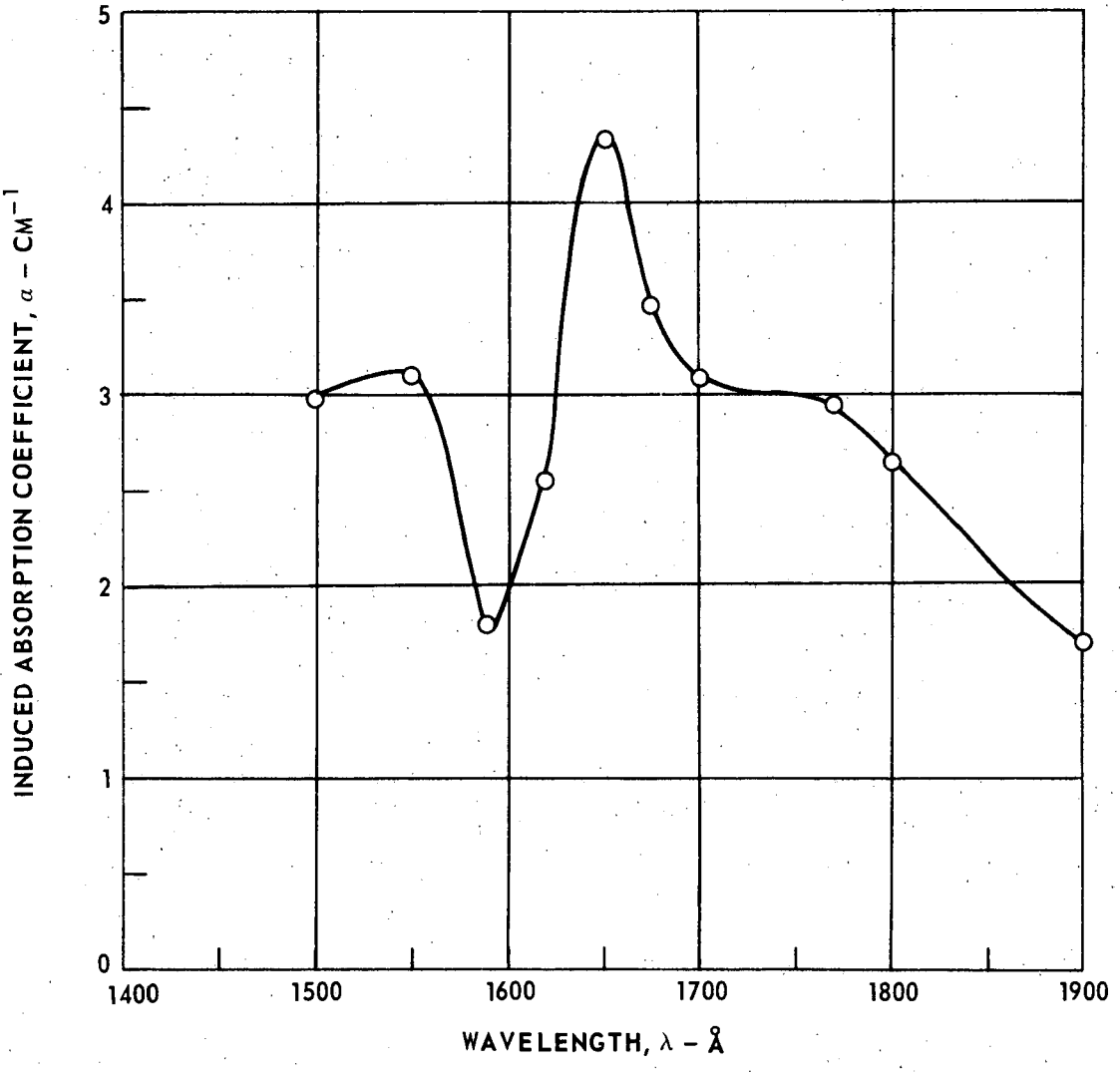

GROWTH OF INDUCED ABSORPTION FOR BERYLLIUM OXIDE SPECIMEN BEO-2 DURING 1.5-MEV ELECTRON IRRADIATION

$\lambda = 2200$ Å

$\dot{D} = 0.07$ MRAD/SEC

$T = 40°C$

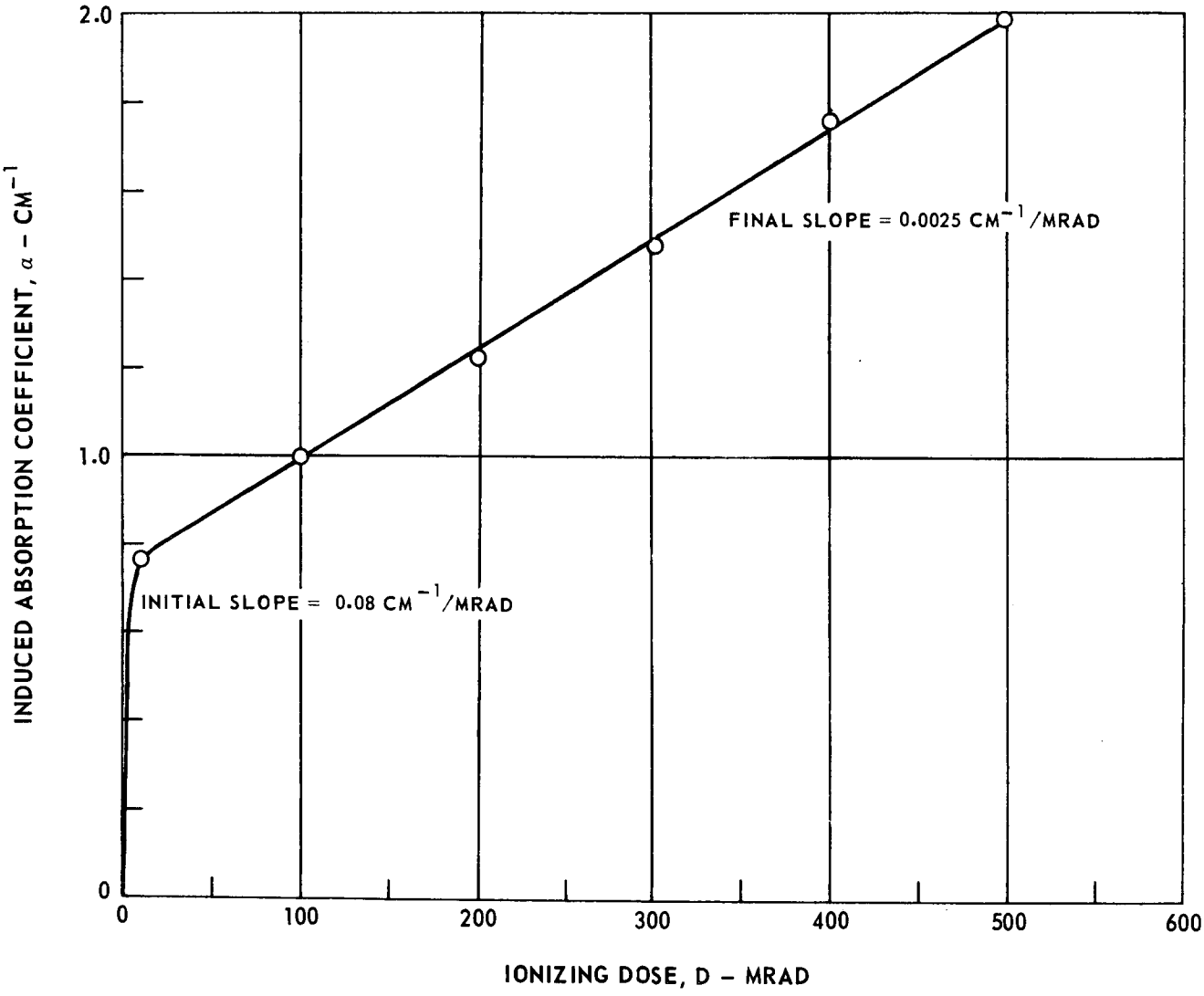

FIG. 7

OPTICAL ABSORPTION IN BERYLLIUM OXIDE SPECIMEN BEO-3 DURING 1.5-MEV ELECTRON IRRADIATION

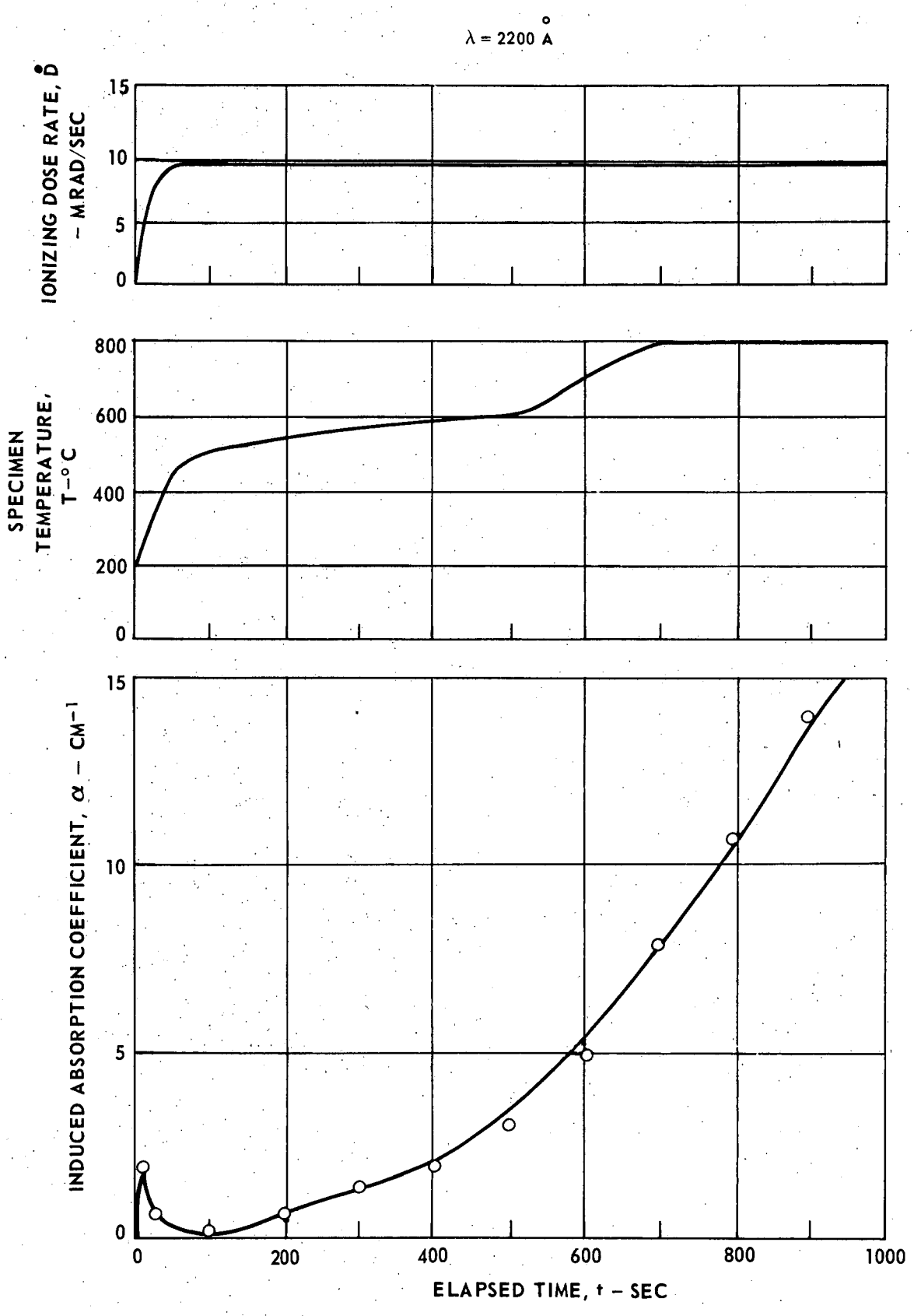

FIG. 8

ABSORPTION SPECTRUM OF BERYLLIUM OXIDE SPECIMEN BEO-3 AFTER HIGH DOSE RATE 1.5-MEV ELECTRON IRRADIATION

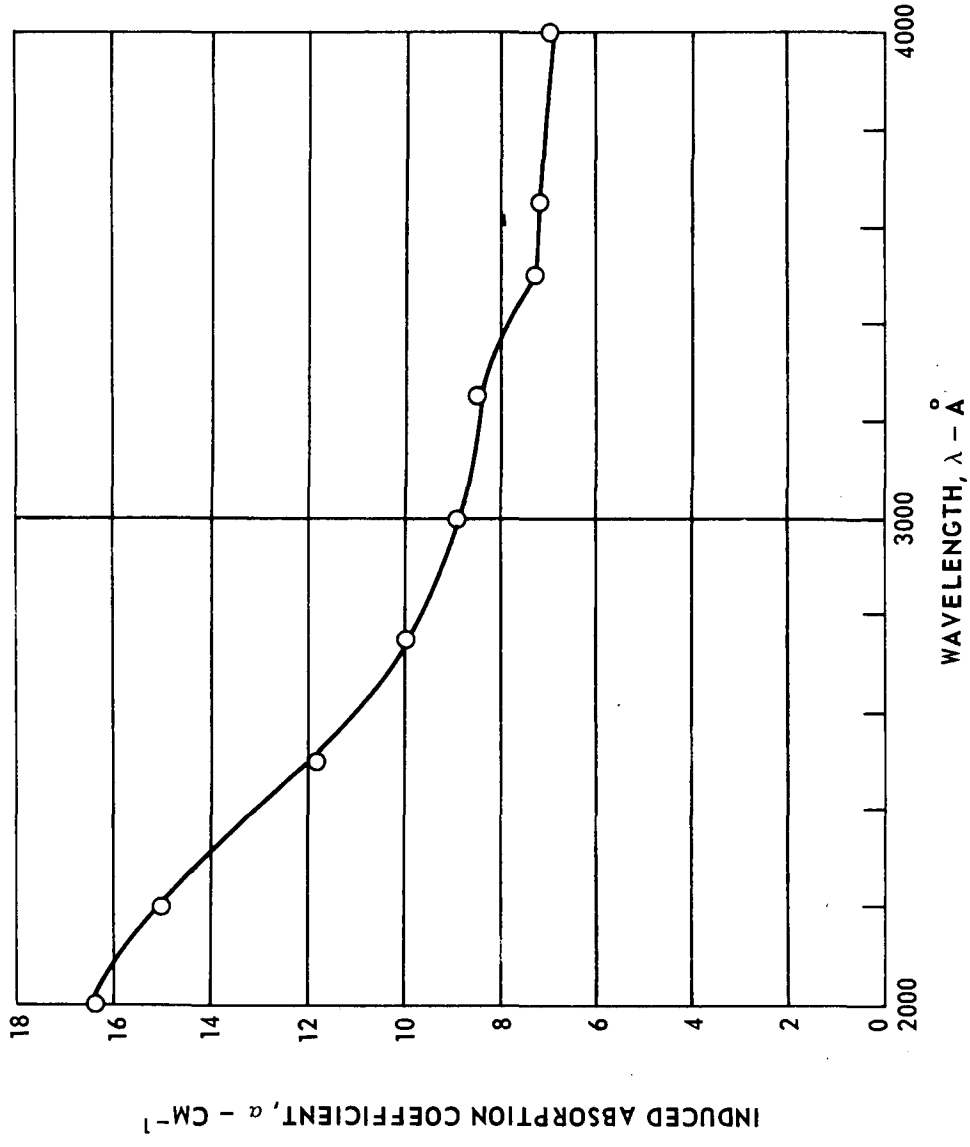

FIG. 9

ABSORPTION SPECTRA OF BERYLLIUM OXIDE SPECIMEN BEO-4 AFTER REACTOR IRRADIATION AND THERMAL ANNEALING

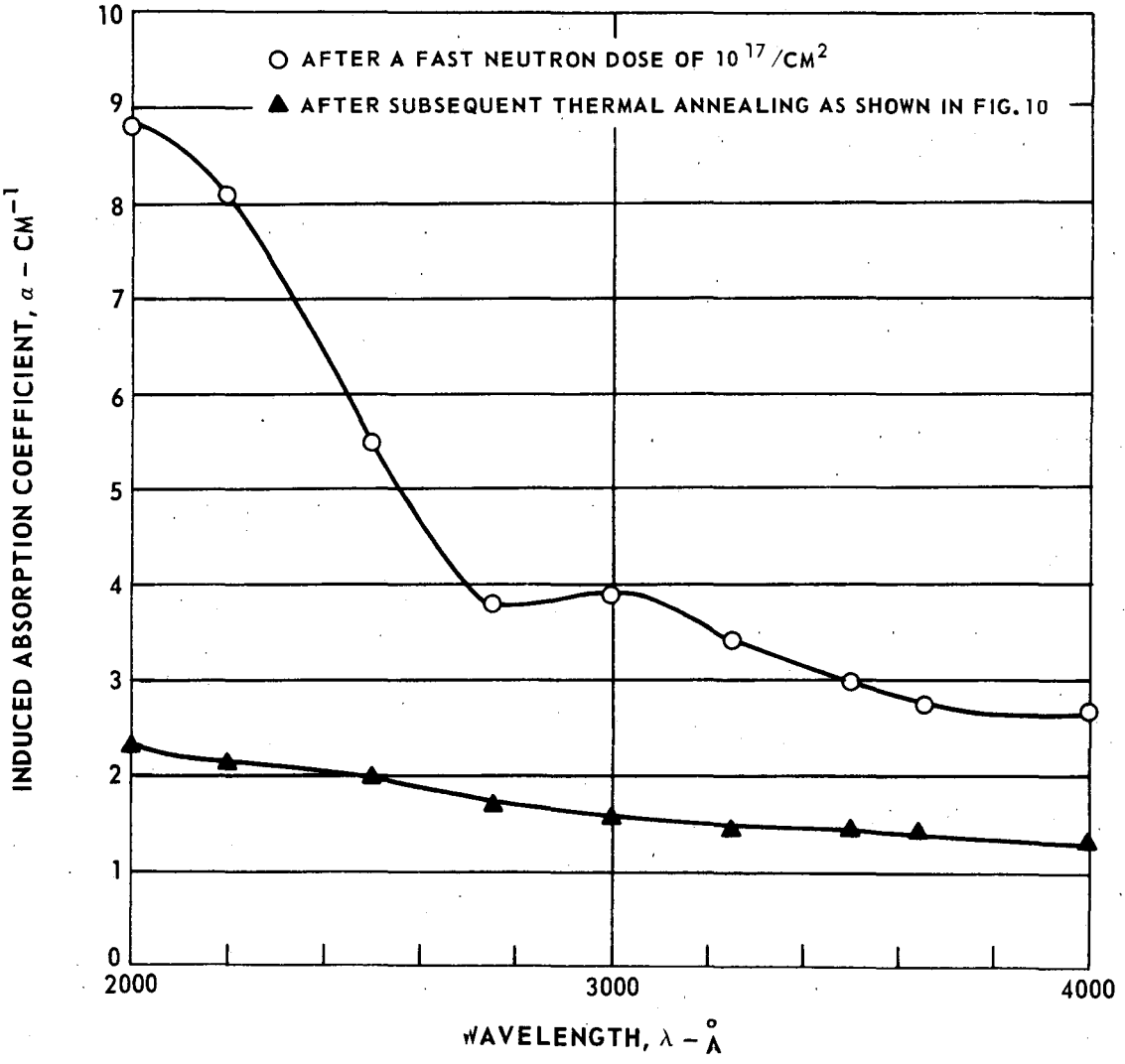

THERMAL ANNEALING OF REACTOR IRRADIATION-INDUCED ABSORPTION IN BERYLLIUM OXIDE SPECIMEN BEO-4

L-990929-3

$\lambda = 2200$ Å

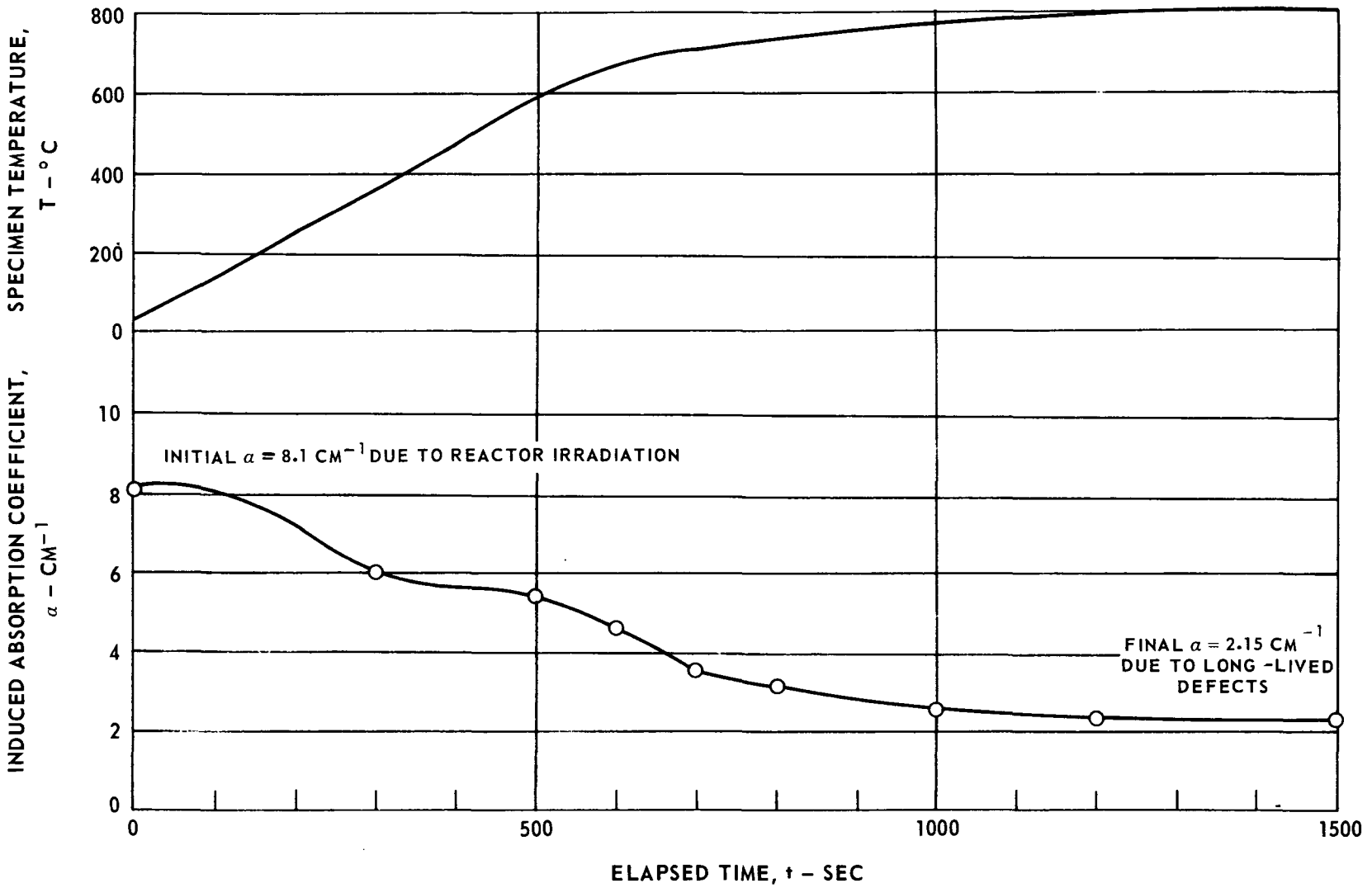

FIG. 10

GROWTH OF INDUCED ABSORPTION IN BERYLLIUM OXIDE DURING ELECTRON IRRADIATION AT SEVERAL ENERGIES

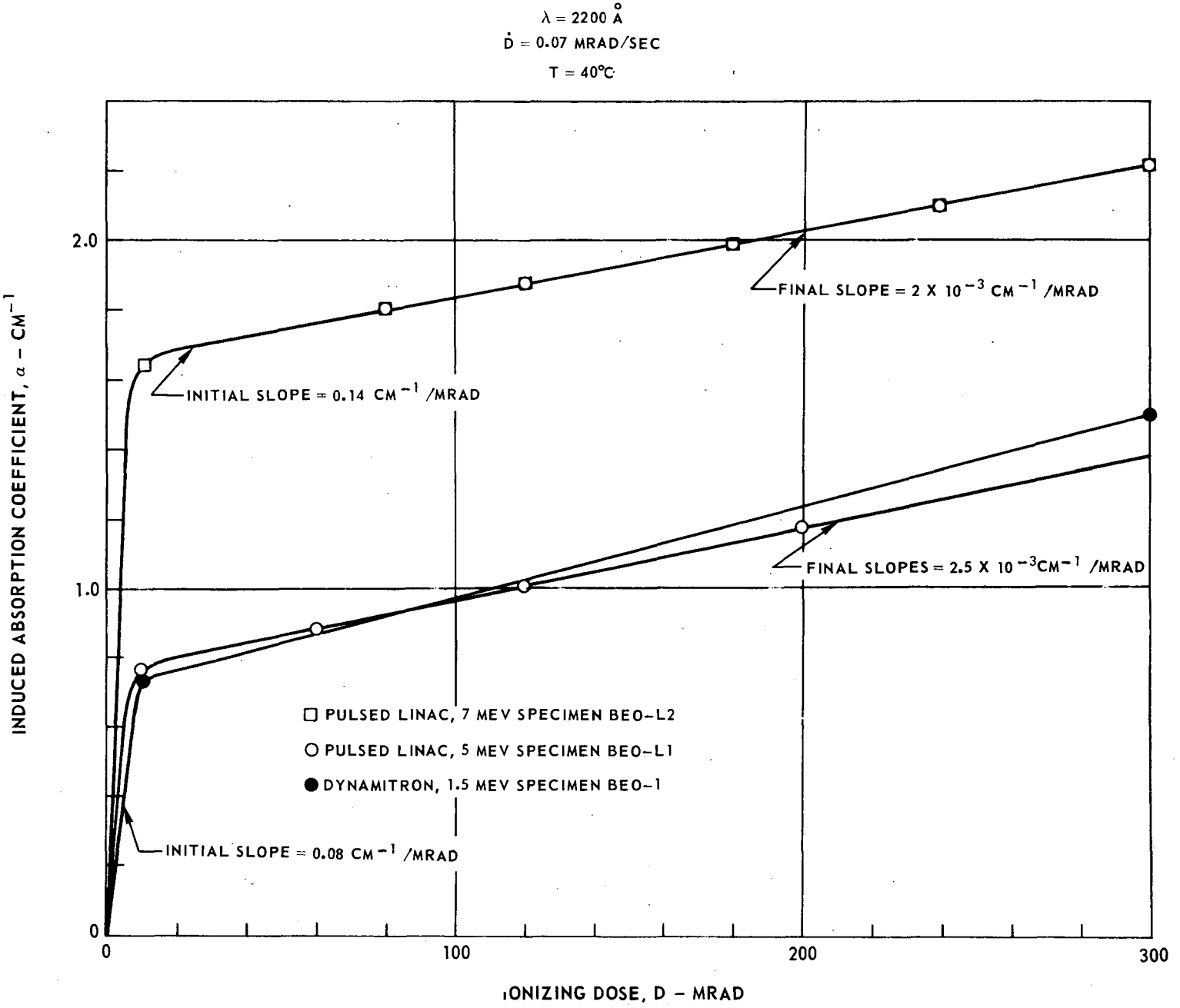

L-990929-3

FIG. 11

L-990929-3

GROWTH OF INDUCED ABSORPTION FOR FUSED SILICA SPECIMEN SV-1 DURING 1.5-MEV ELECTRON IRRADIATION

$\lambda = 1900$ Å

$\dot{D} = 0.5$ MRAD/SEC

T = 40°C

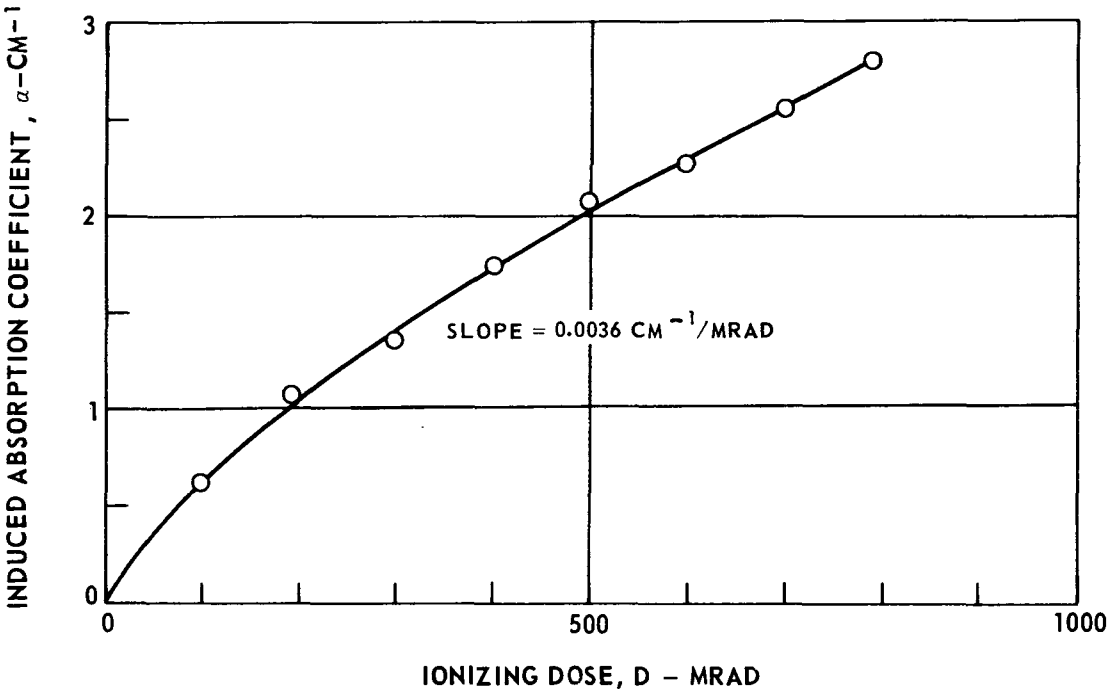

FIG. 12

FIG. 13

VACUUM UV ABSORPTION SPECTRA OF FUSED SILICA SPECIMEN SV-1 FOLLOWING 1.5-MEV ELECTRON IRRADIATION AND RADIATION ANNEALING

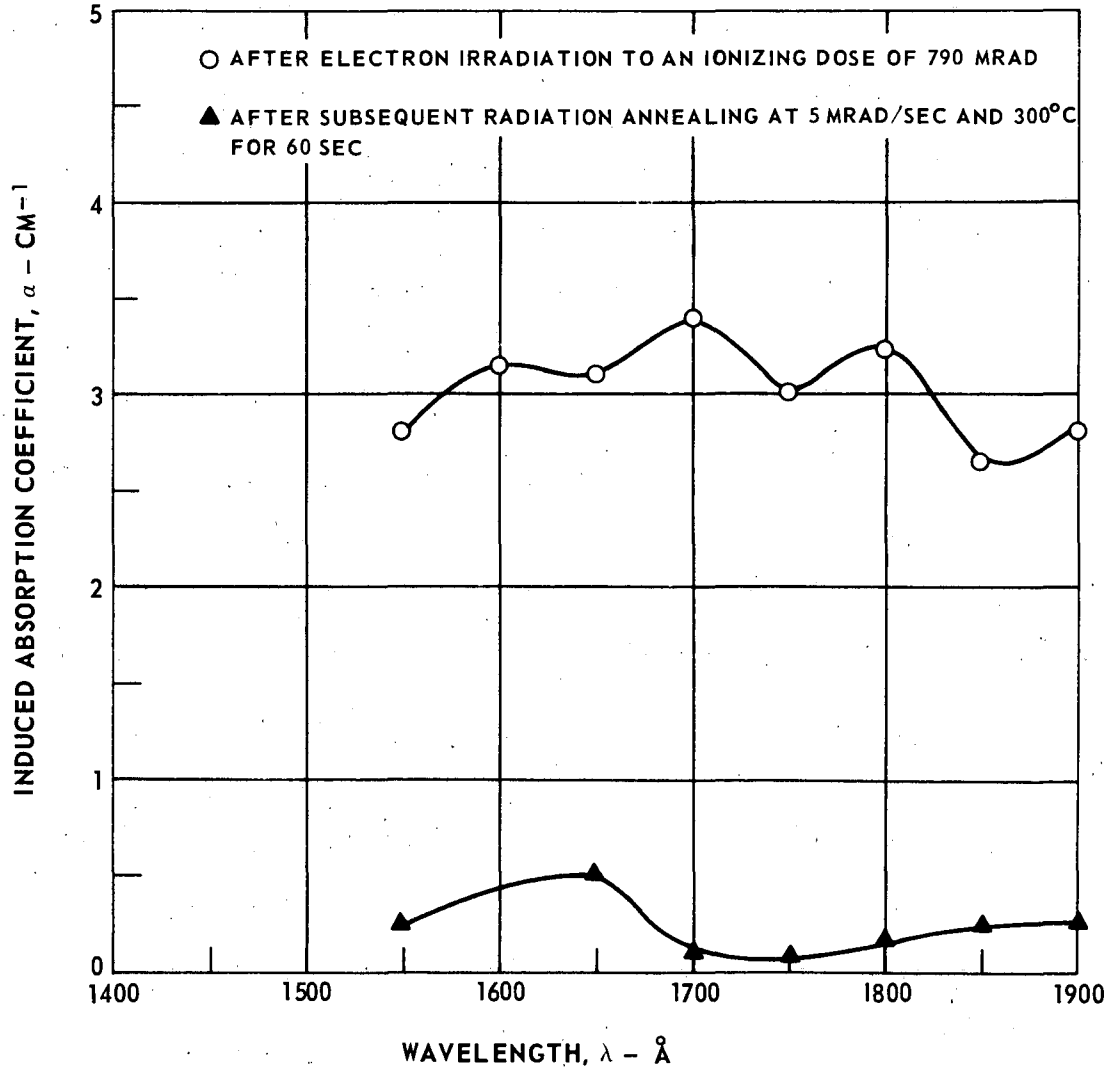

FIG. 14

GROWTH OF INDUCED ABSORPTION FOR FUSED SILICA SPECIMEN SV-2 DURING 1.5-MEV ELECTRON IRRADIATION

$\lambda = 1800$ Å

$\dot{D} = 0.5$ MRAD/SEC

$T = 40°C$

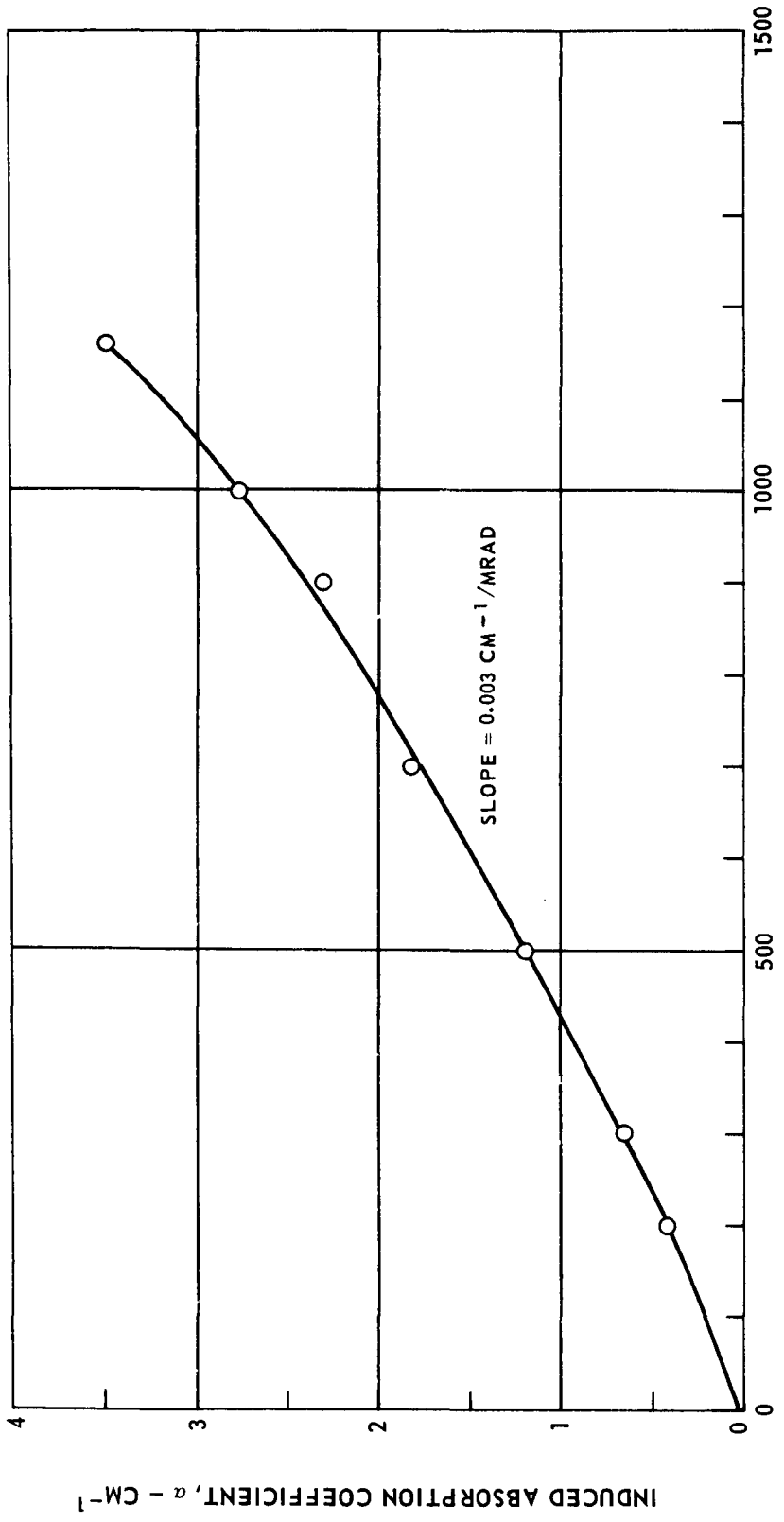

FIG. 15

VACUUM UV ABSORPTION SPECTRA OF FUSED SILICA SPECIMEN SV-2 FOLLOWING 1.5-MEV ELECTRON IRRADIATION AND OPTICAL BLEACHING

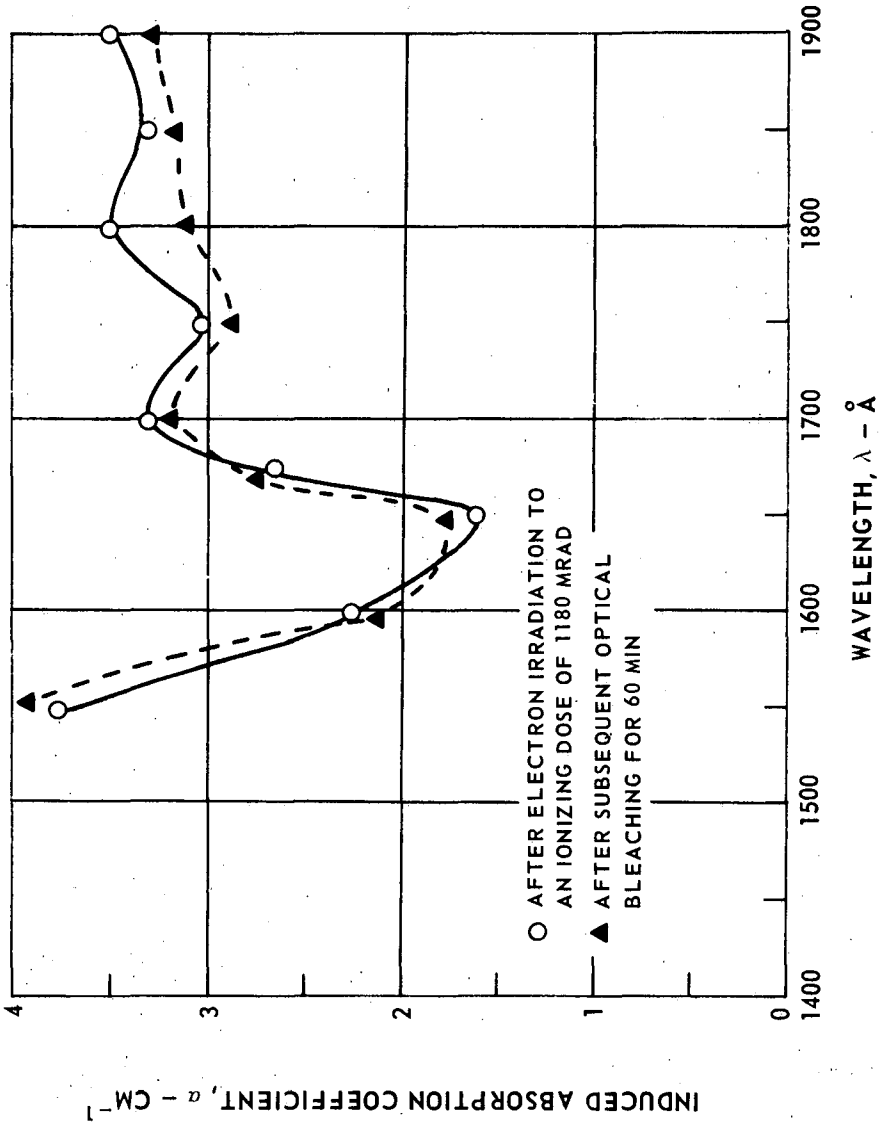

L-990929-3

GROWTH OF INDUCED ABSORPTION FOR FUSED SILICA SPECIMEN SV-3 DURING 1.5-MEV ELECTRON IRRADIATION

$\lambda = 1650$ Å

$\dot{D} = 0.25$ MRAD/SEC

$T = 40°C$

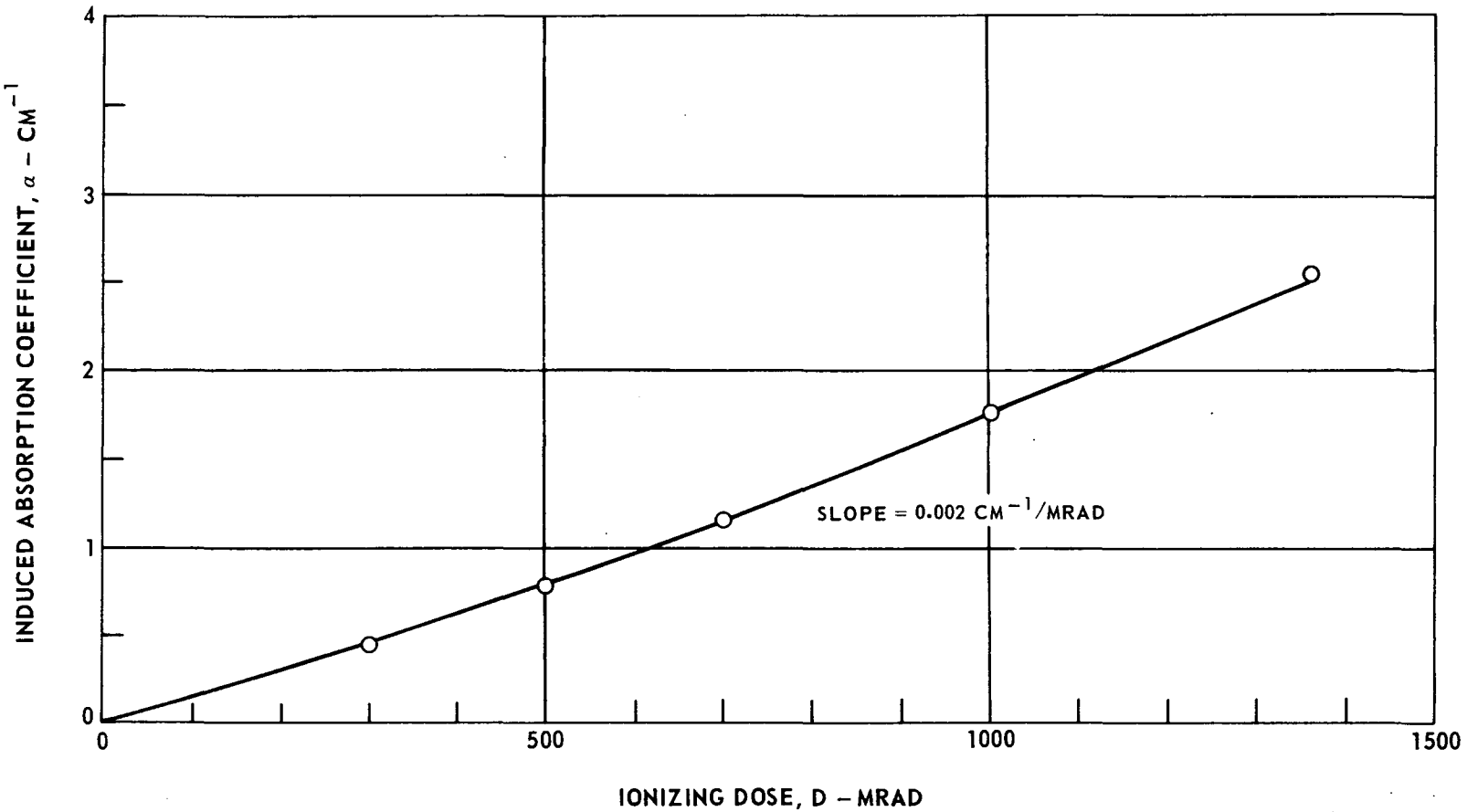

FIG. 16

FIG. 17

VACUUM UV ABSORPTION SPECTRA OF FUSED SILICA SPECIMEN SV-3 FOLLOWING 1.5 - MEV ELECTRON IRRADIATION AND THERMAL ANNEALING

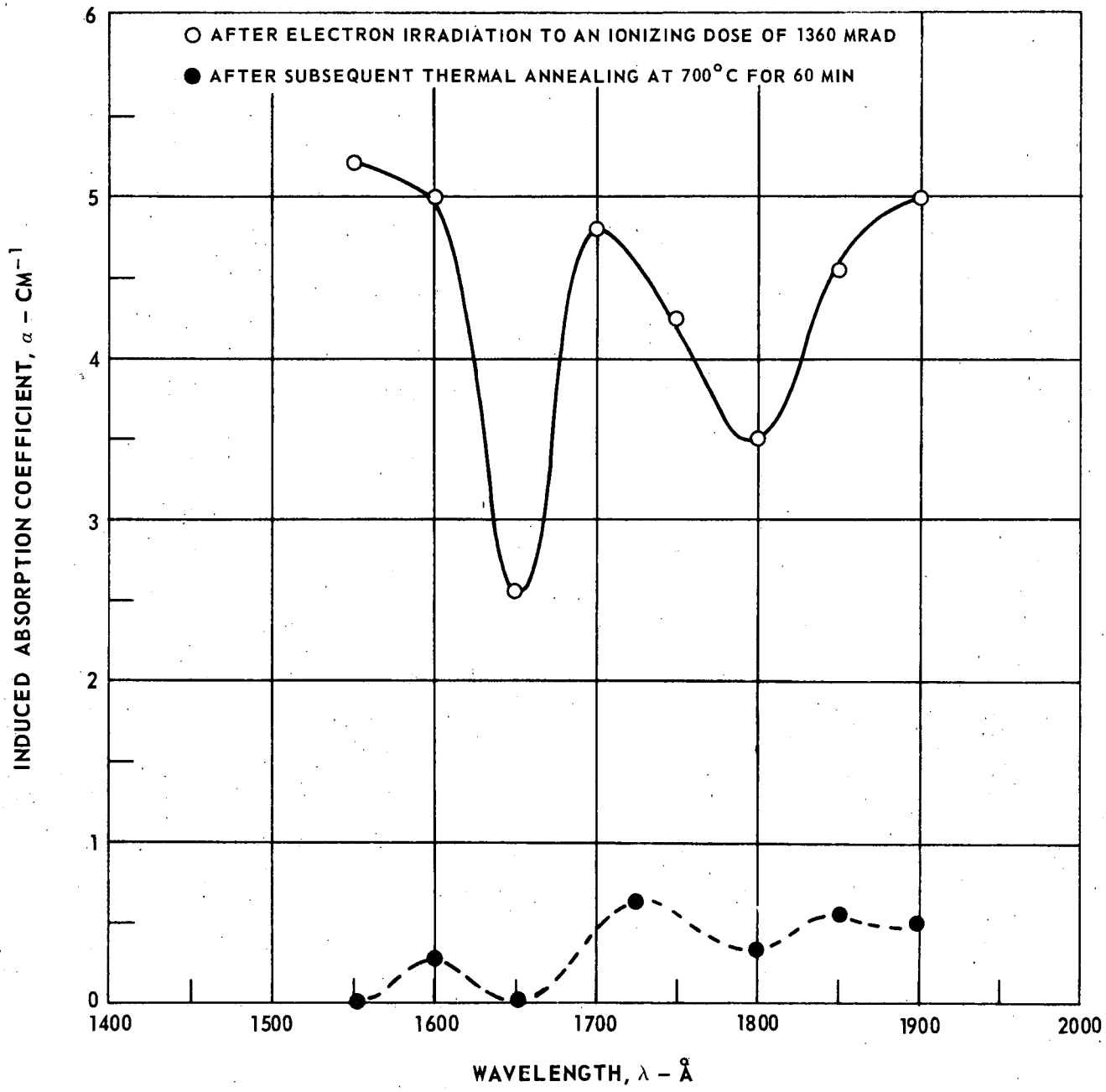

FIG. 18

VACUUM UV ABSORPTION SPECTRA OF FUSED SILICA SPECIMEN SVN-1
FOLLOWING REACTOR IRRADIATION AND THERMAL ANNEALING

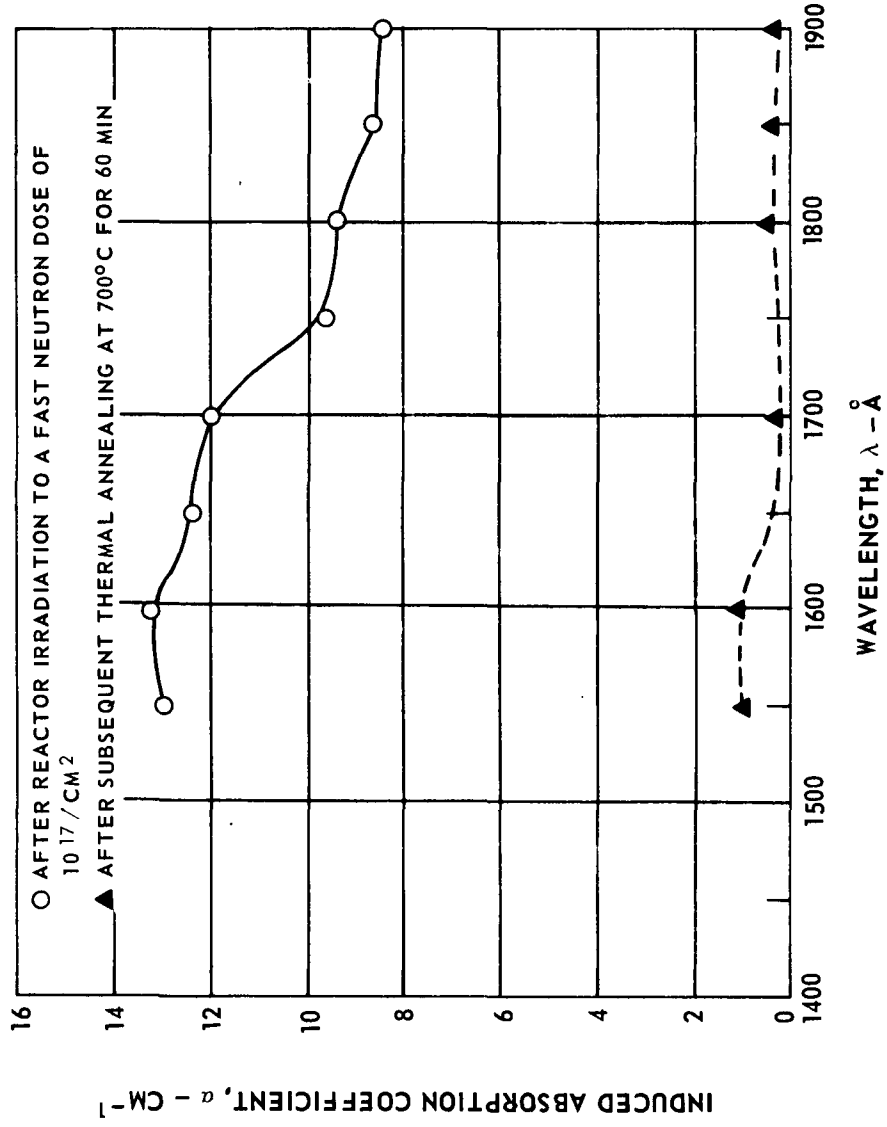

FIG. 19

RADIATION ANNEALING OF FUSED SILICA SPECIMEN SCN-1 DURING 1.5-MEV ELECTRON IRRADIATION

$\lambda = 2150$ Å

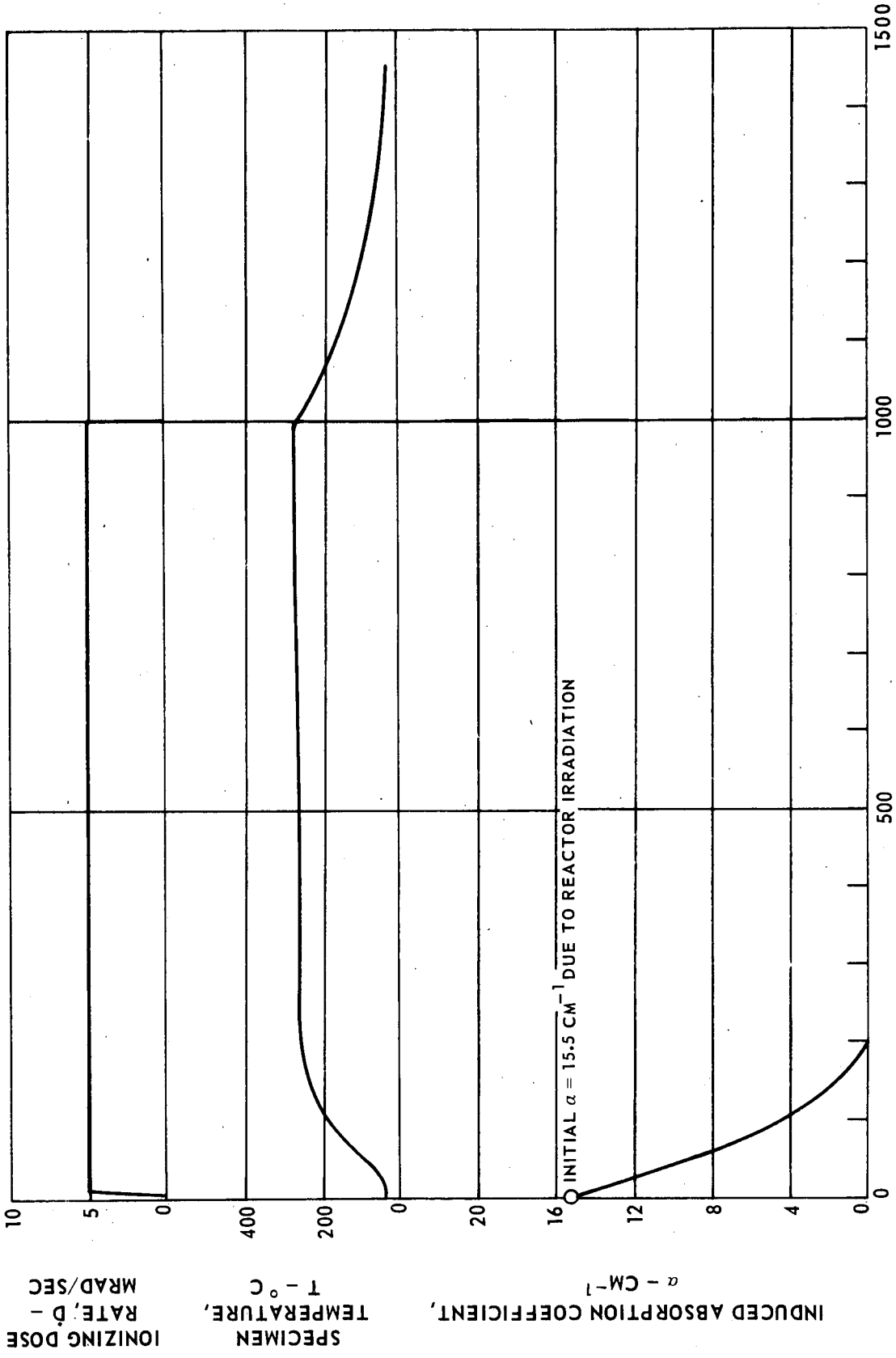

RADIATION ANNEALING OF FUSED SILICA SPECIMEN SCN-2 DURING 1.5-MEV ELECTRON IRRADIATION

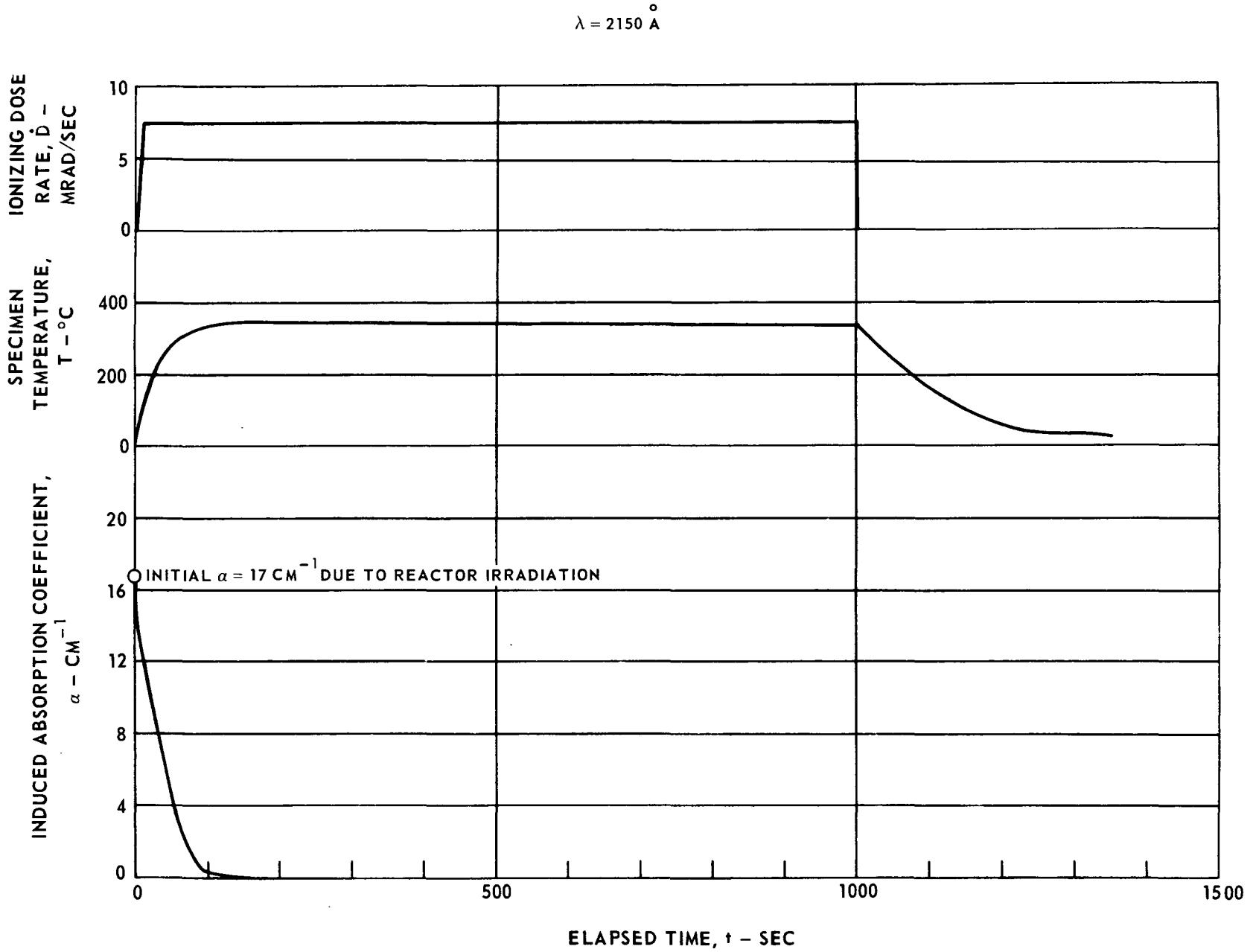

L-990929-3

FIG. 20

FIG. 21

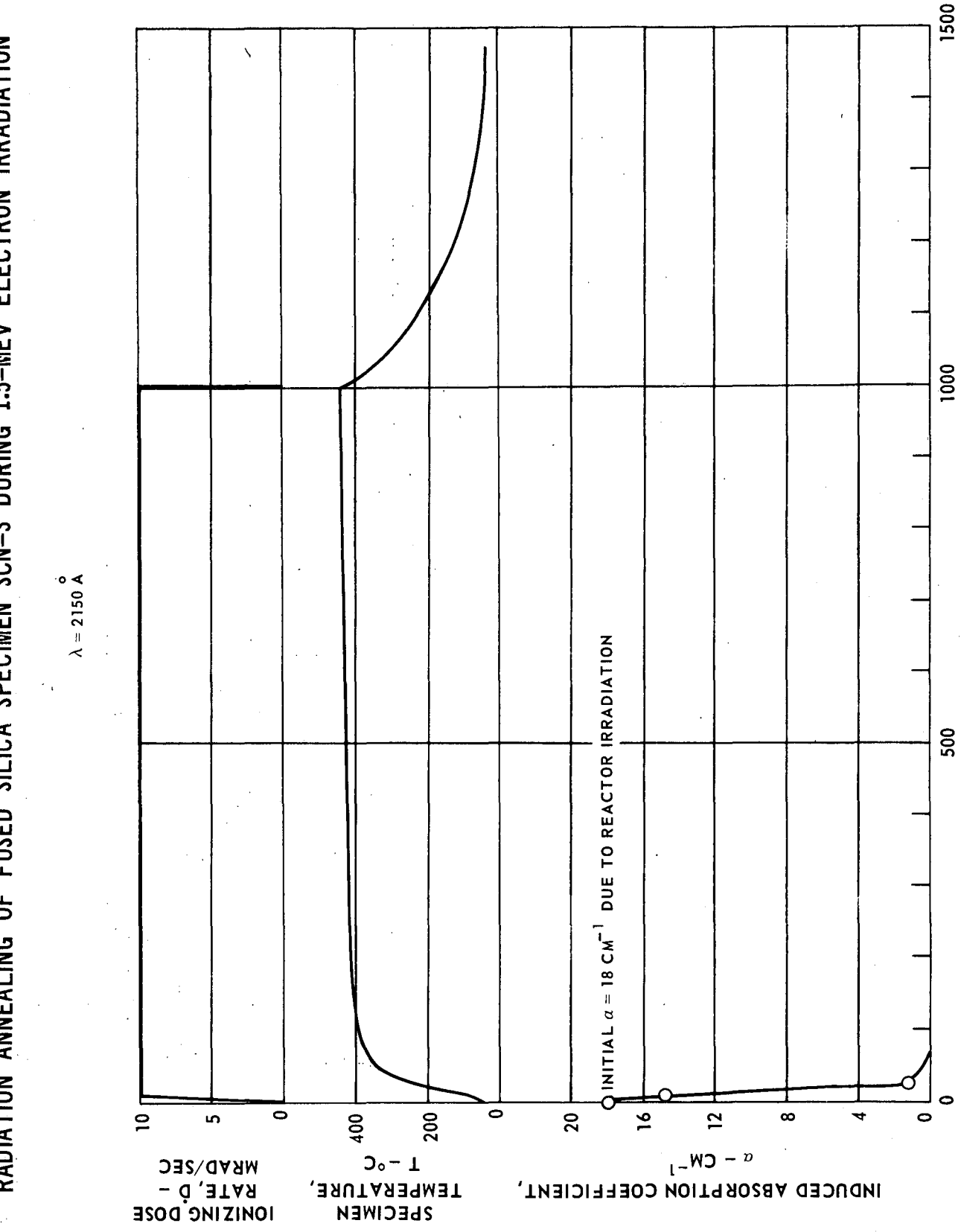
RADIATION ANNEALING OF FUSED SILICA SPECIMEN SCN-3 DURING 1.5-MEV ELECTRON IRRADIATION
λ = 2150 Å
INDUCED ABSORPTION COEFFICIENT, α - CM⁻¹
SPECIMEN TEMPERATURE, T - °C
IONIZING DOSE RATE, Ḋ - MRAD/SEC
INITIAL α = 18 CM⁻¹ DUE TO REACTOR IRRADIATION
ELAPSED TIME, t - SEC
0
4
8
12
16
20
0
200
400
0
5
10
0
500
1000
1500

FIG. 22

GROWTH OF INDUCED ABSORPTION FOR CORNING SPECIMEN SL-1 DURING 5-MEV PULSED LINAC IRRADIATION

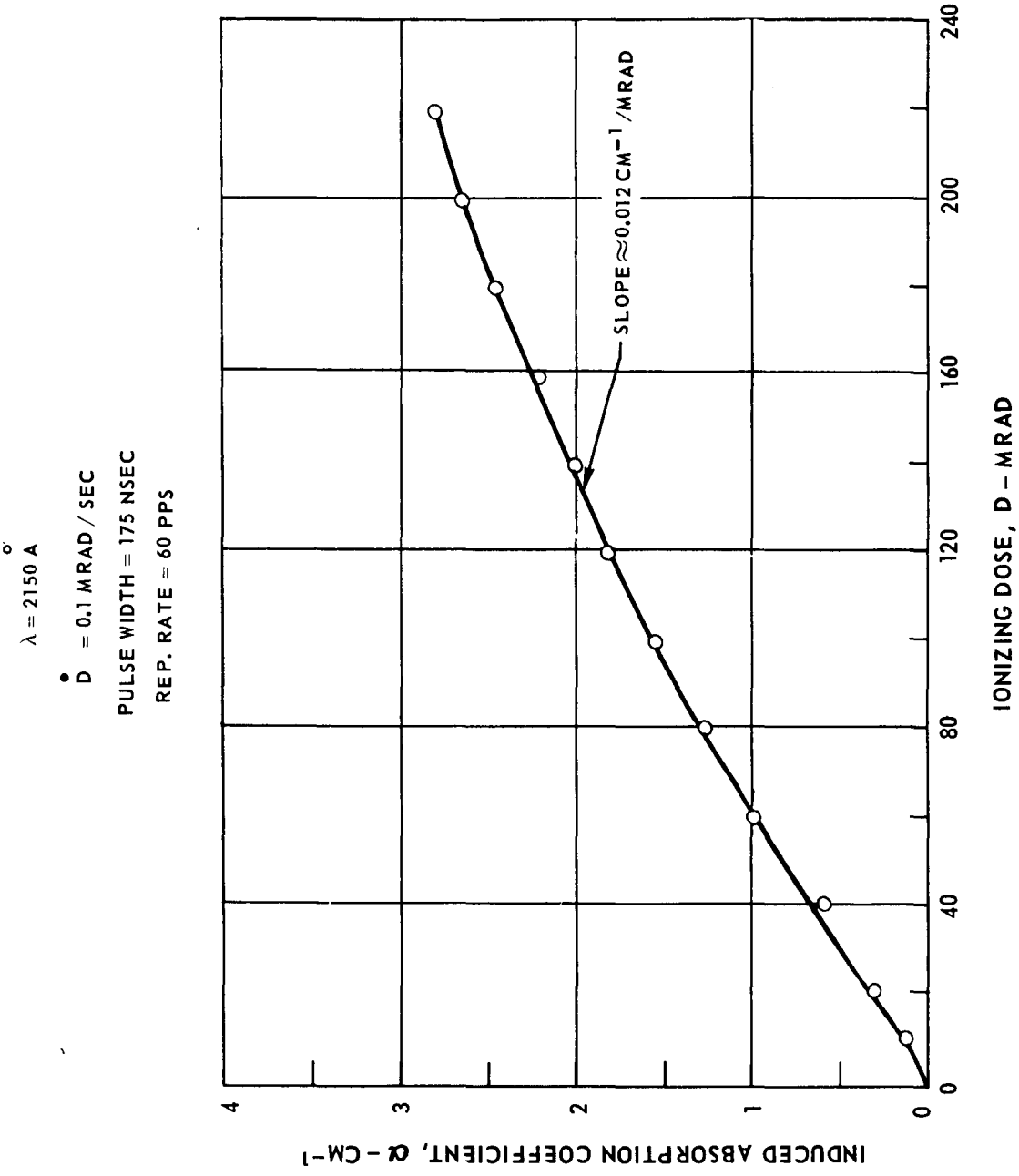

VARIATION OF INDUCED ABSORPTION FOR CORNING SPECIMEN SL-2 DURING 7-MEV PULSED LINAC IRRADIATION

$\lambda = 2150$ Å

PULSE WIDTH = 0.5 μ SEC

REP. RATE = 120 PPS

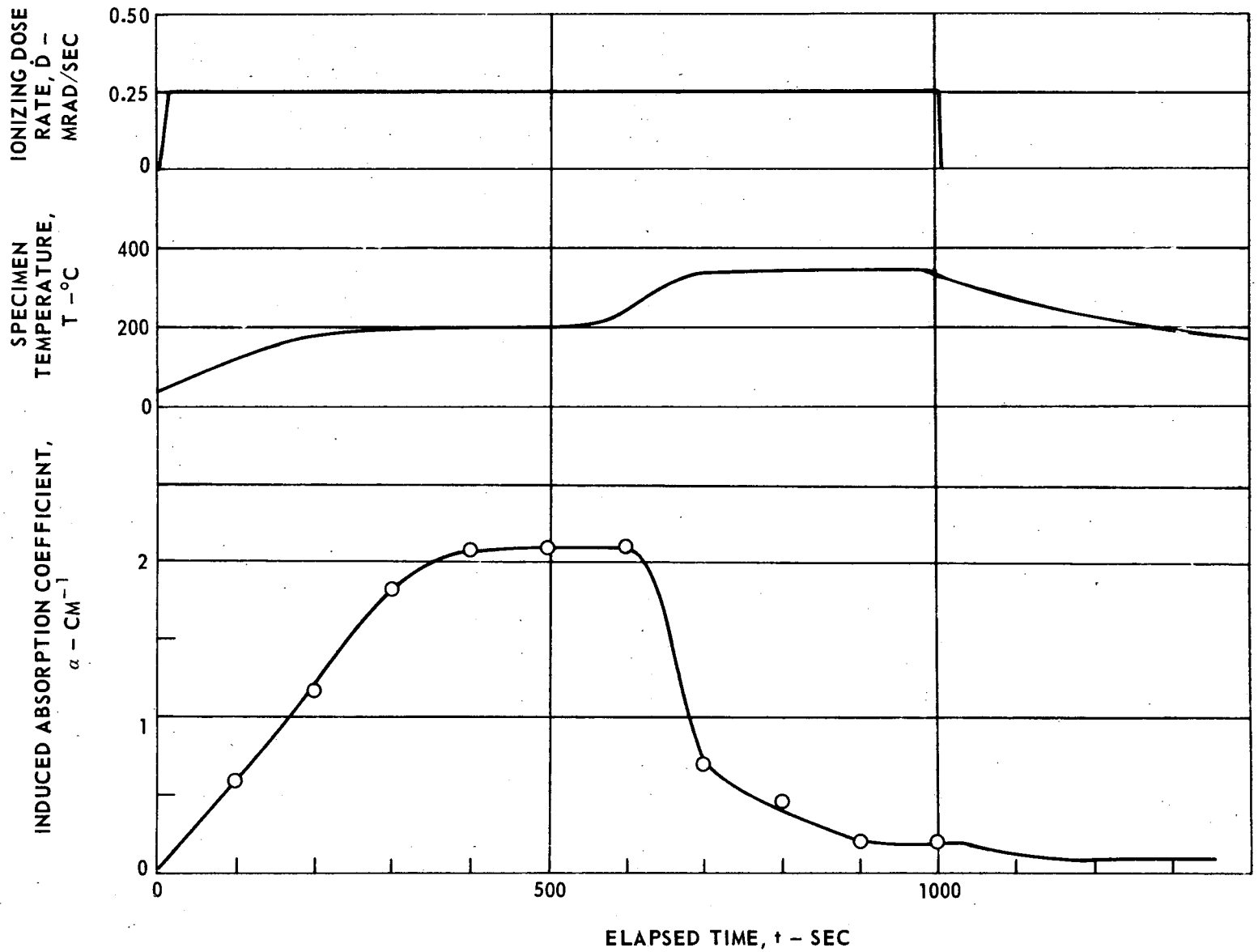

L-990929-3

FIG. 23

VARIATION OF INDUCED ABSORPTION FOR CORNING SPECIMEN SL-3 DURING 7-MEV PULSED LINAC IRRADIATION

λ = 2150 Å

PULSE WIDTH = 0.5 μ SEC

REP. RATE = 240 PPS

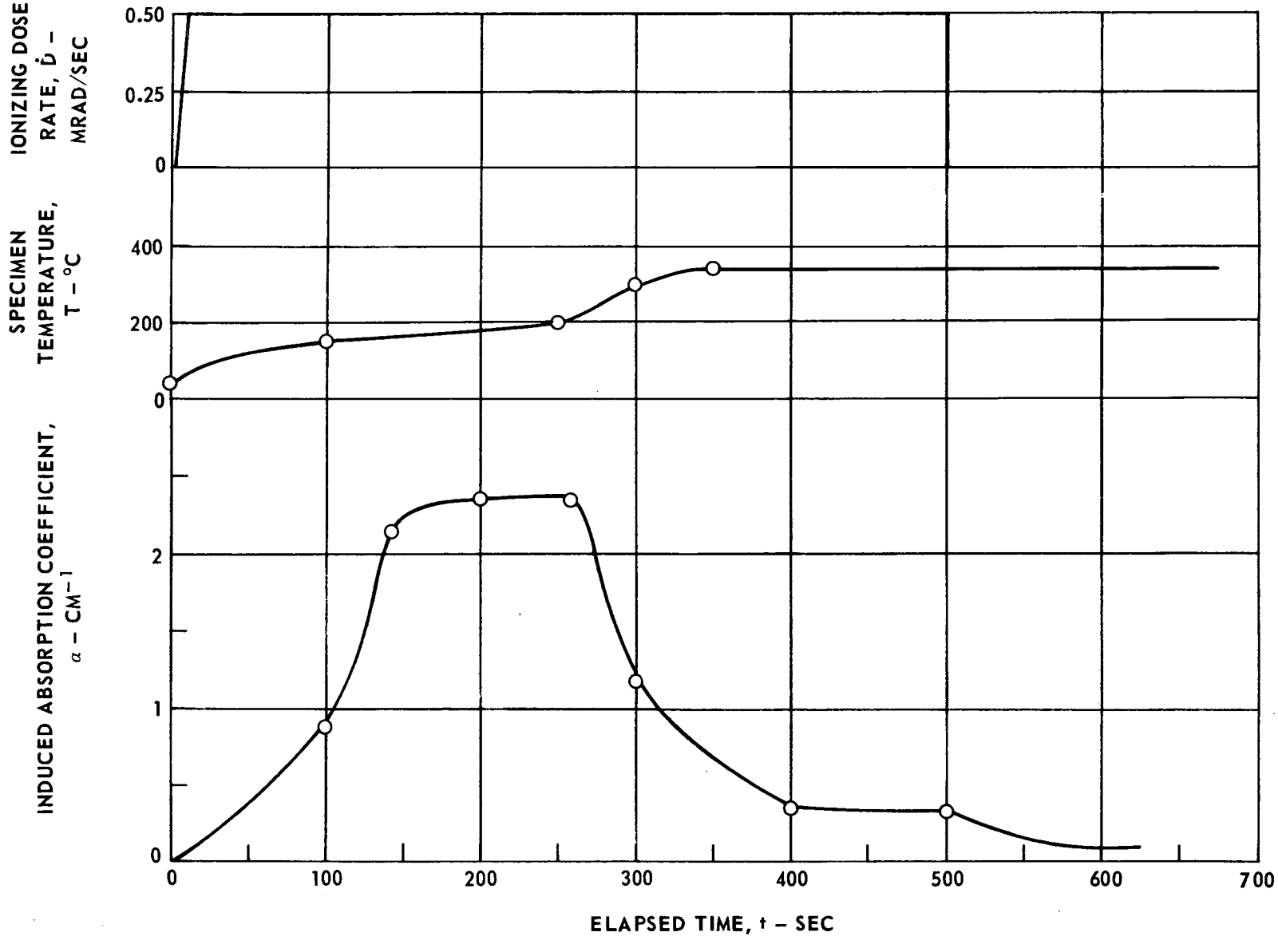

L-990929-3

FIG. 24

VARIATION OF INDUCED ABSORPTION FOR CORNING SPECIMEN SL-4 DURING 7-MEV PULSED LINAC IRRADIATION

$\lambda = 2150$ Å

PULSE WIDTH = 0.5 μ SEC

REP. RATE = 360 PPS

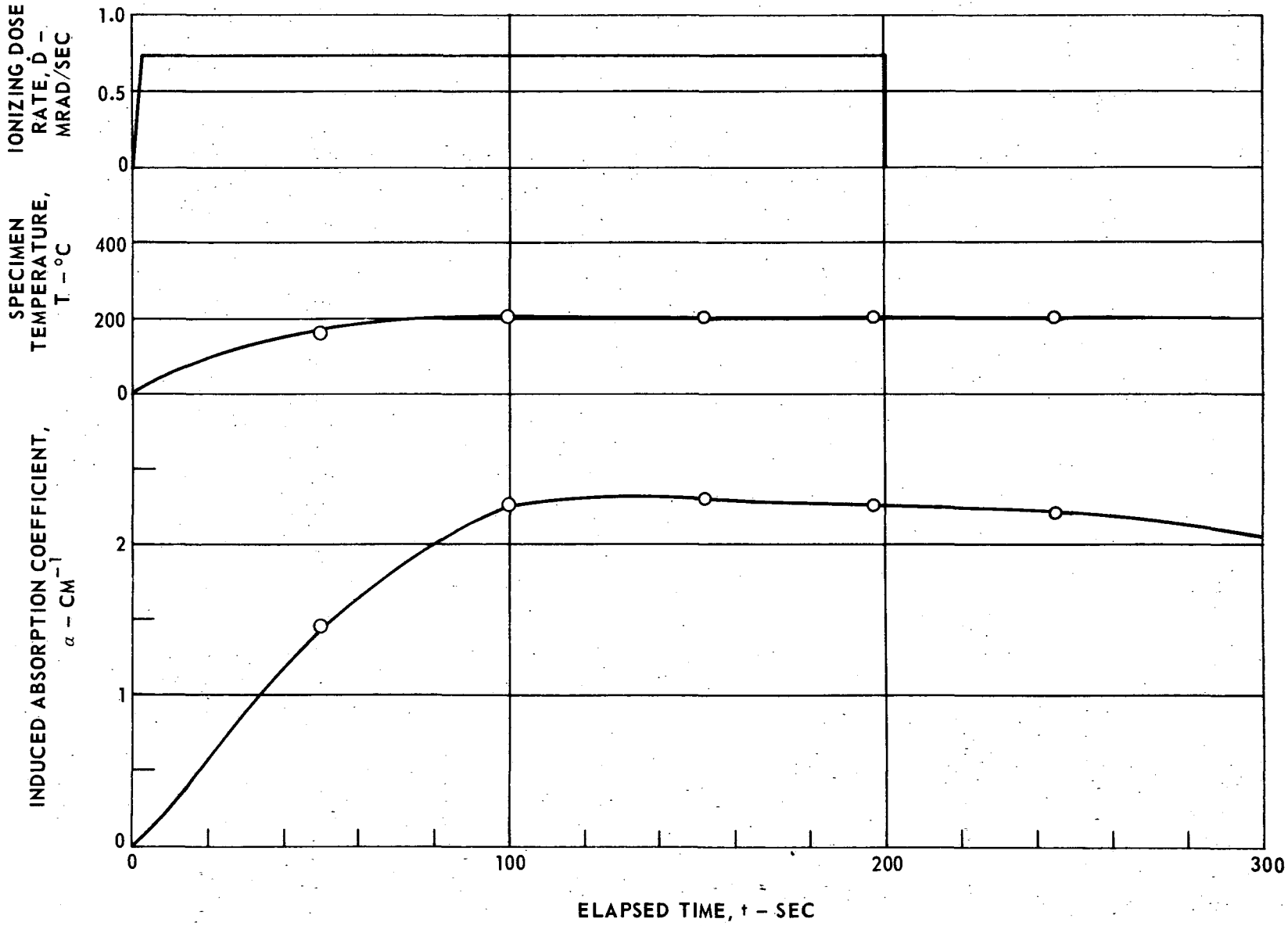

L-990929-3

FIG. 25

FIG. 26

GROWTH OF INDUCED ABSORPTION FOR MgF_2 SPECIMEN DURING 1.5-MEV ELECTRON IRRADIATION

$\lambda = 1800$ Å

$\dot{D} = 0.1$ MRAD/SEC

$T = 40°C$

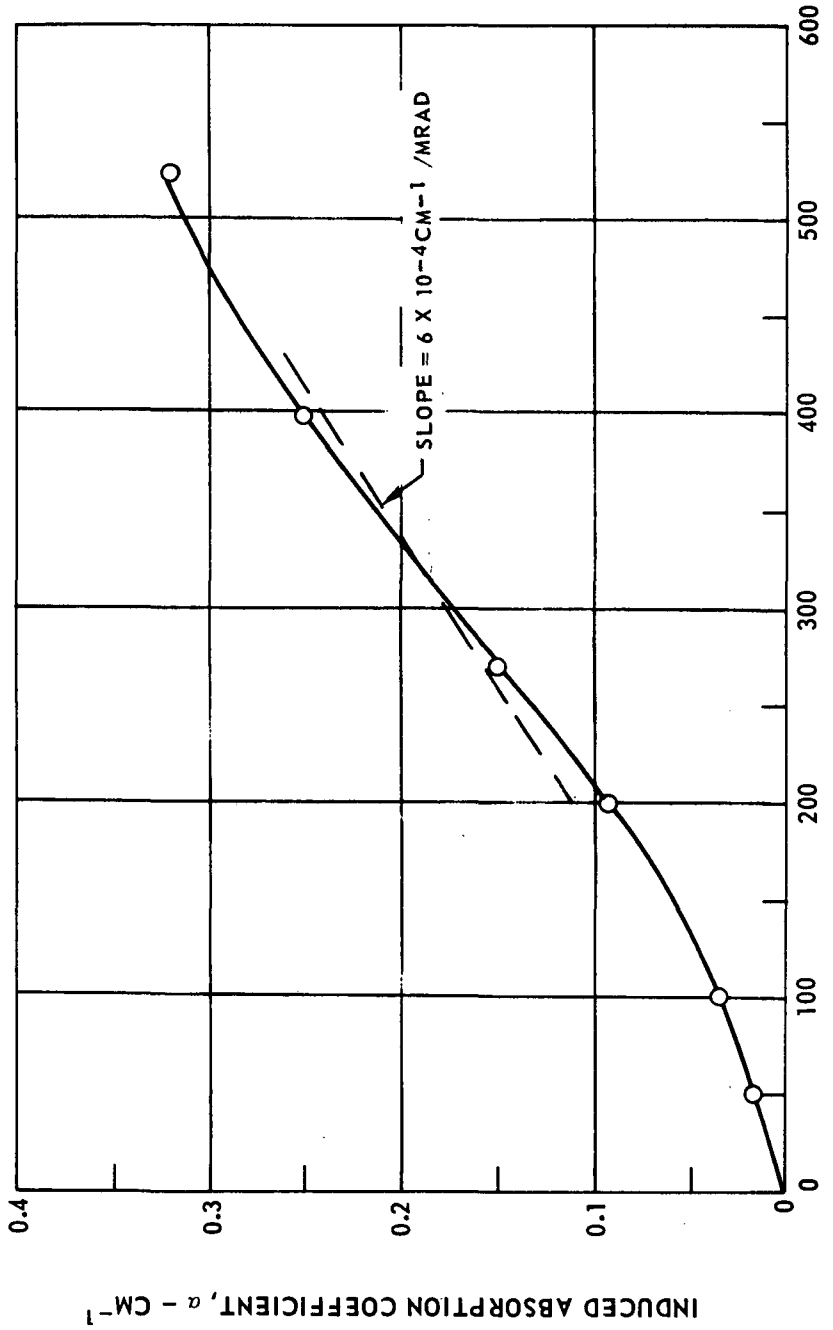

FIG. 27

VACUUM UV ABSORPTION SPECTRUM OF MgF_2 SPECIMEN FOLLOWING 1.5-MEV ELECTRON IRRADIATION

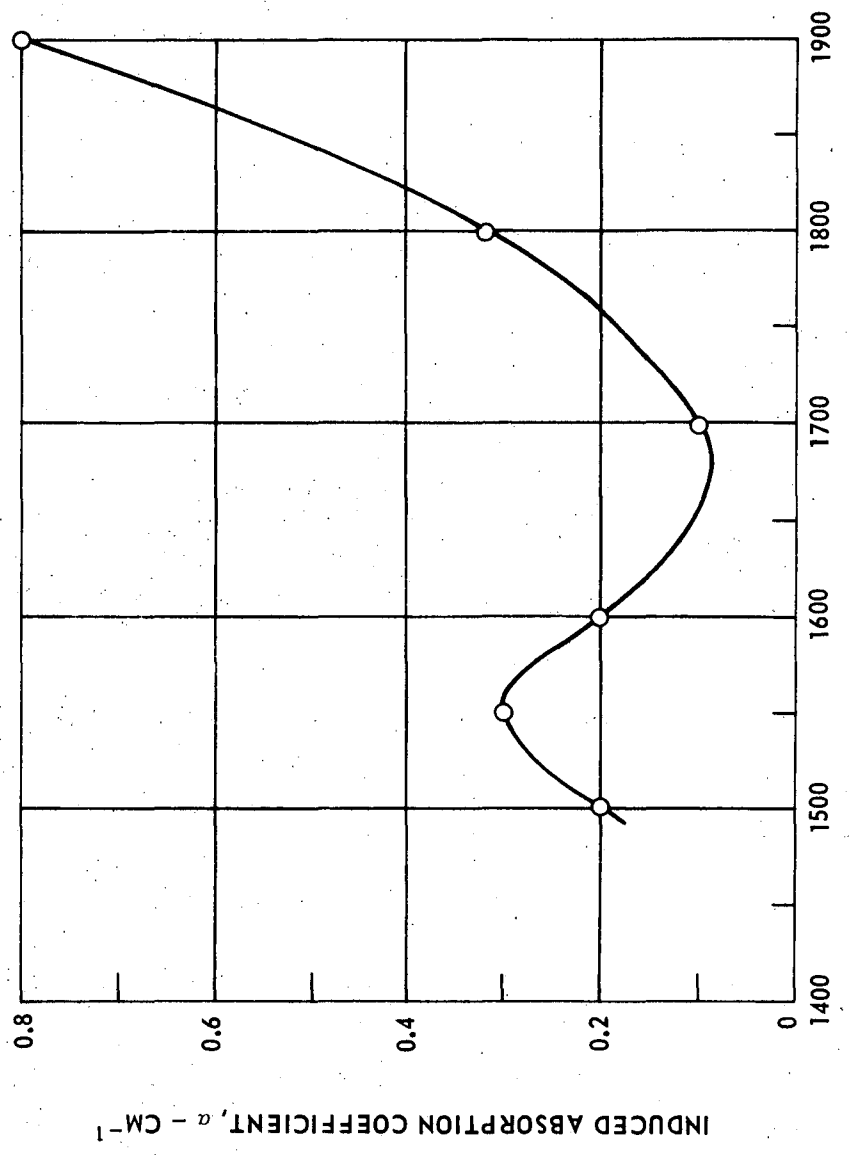

GROWTH OF INDUCED ABSORPTION FOR LiF SPECIMEN DURING 1.5-MEV ELECTRON IRRADIATION

λ = 1800 Å

$\dot{D}$ = 0.1 MRAD/SEC

T = 40°C

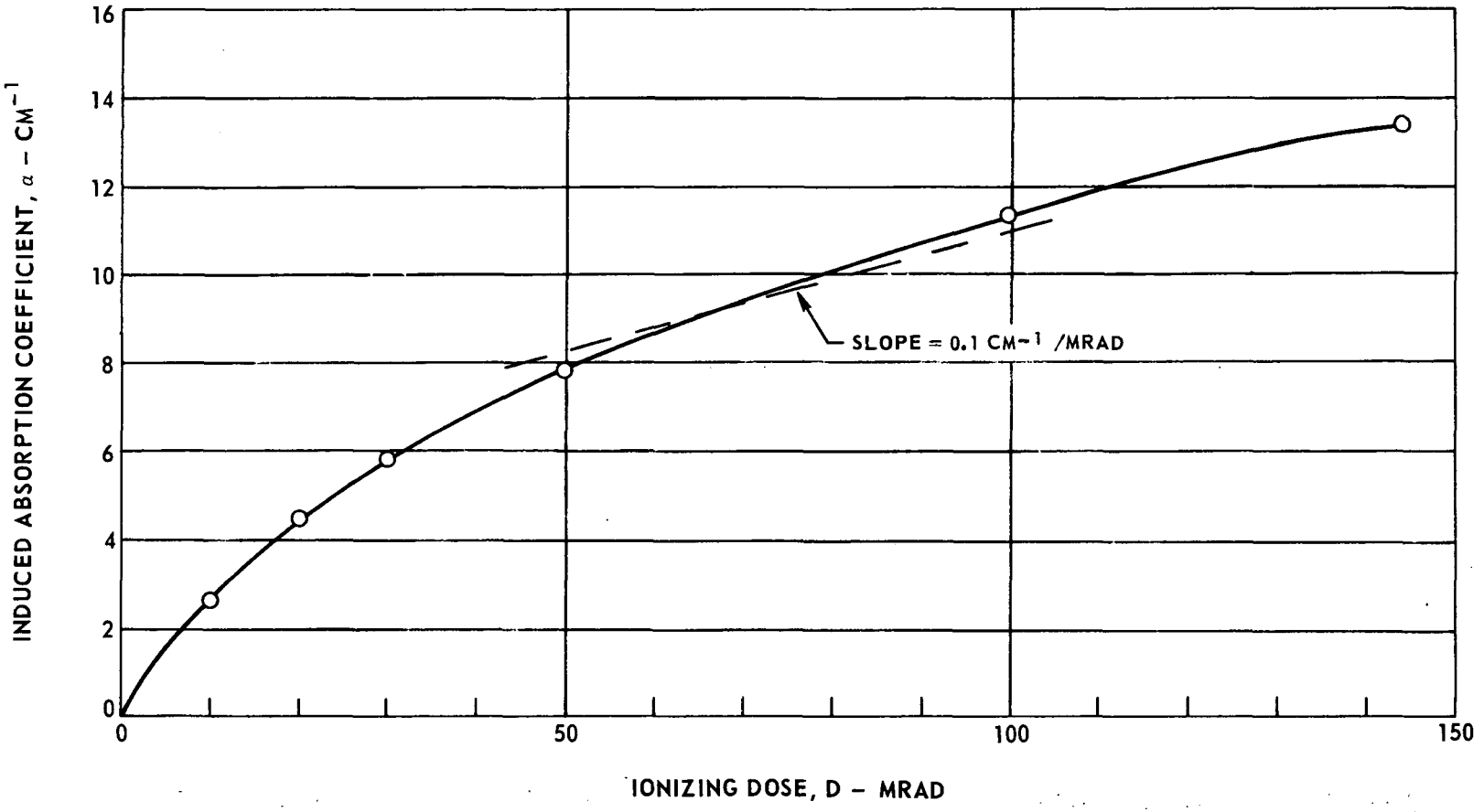

FIG. 28

FIG. 29

VACUUM UV ABSORPTION SPECTRUM OF LiF SPECIMEN FOLLOWING 1.5-MEV ELECTRON IRRADIATION

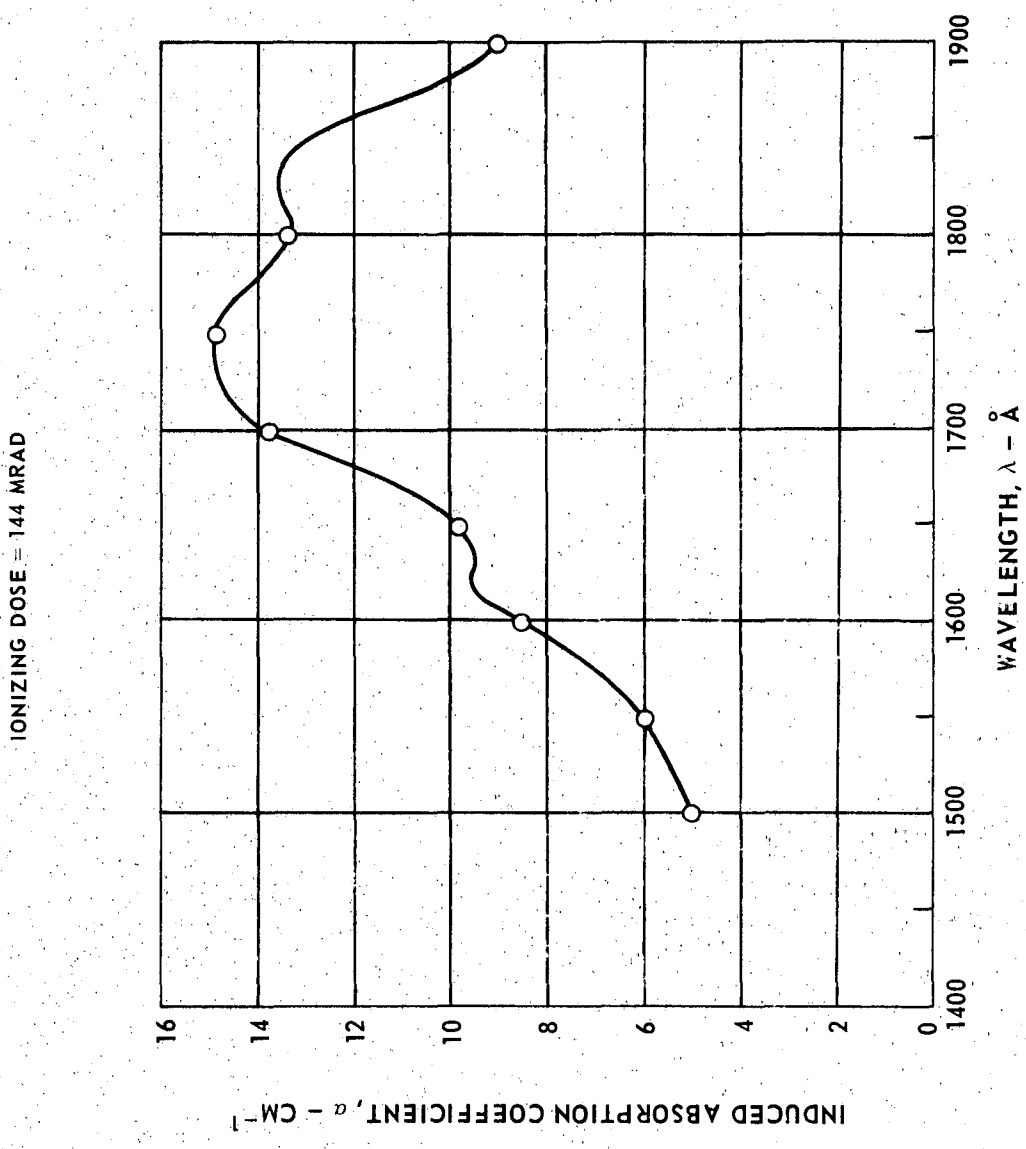

FIG. 30

THERMOCOUPLE LOCATION FOR ELECTRON IRRADIATION EXPERIMENTS

r_e = ELECTRON BEAM RADIUS

r_ℓ = LIGHT BEAM RADIUS